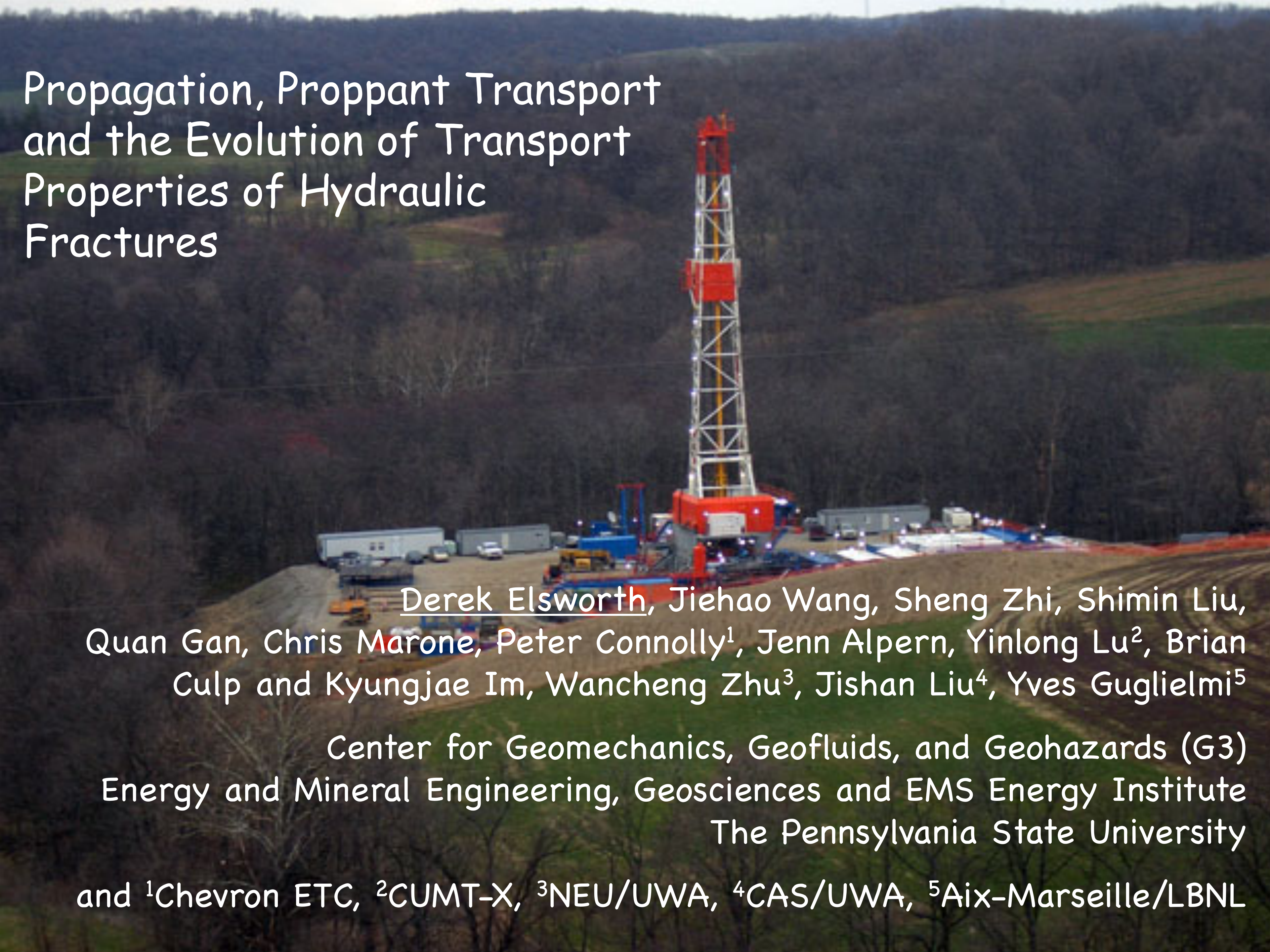

Propagation, Proppant Transport and the Evolution of Transport Properties of Hydraulic Fractures

Derek Elsworth, Jiehao Wang, Sheng Zhi, Shimin Liu, Quan Gan, Chris Marone, Peter Connolly[1], Jenn Alpern, Yinlong Lu[2], Brian Culp and Kyungjae Im, Wancheng Zhu[3], Jishan Liu[4], Yves Guglielmi[5]

Center for Geomechanics, Geofluids, and Geohazards (G3)
Energy and Mineral Engineering, Geosciences and EMS Energy Institute
The Pennsylvania State University

and [1]Chevron ETC, [2]CUMT-X, [3]NEU/UWA, [4]CAS/UWA, [5]Aix-Marseille/LBNL

Some Key Issues in Hydraulic Fracturing

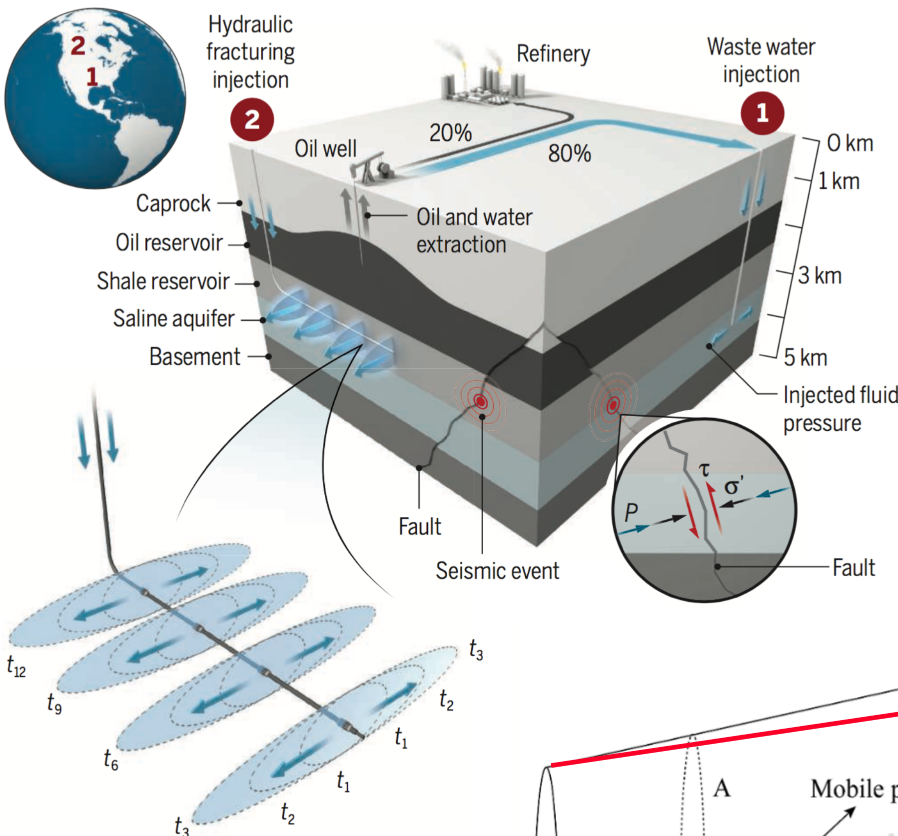

[Elsworth et al., Science, 2016]

How Can We:

Maximize Recovery:

1. Longest/tallest/widest?
2. Highest proppant charge?
3. Most complex?
4. Best matched fluids?
5. Utilize natural natural fracture network?

Minimize Environmental Impacts:

1. Induced seismicity
2. Post treatment of flowback (NORMs)

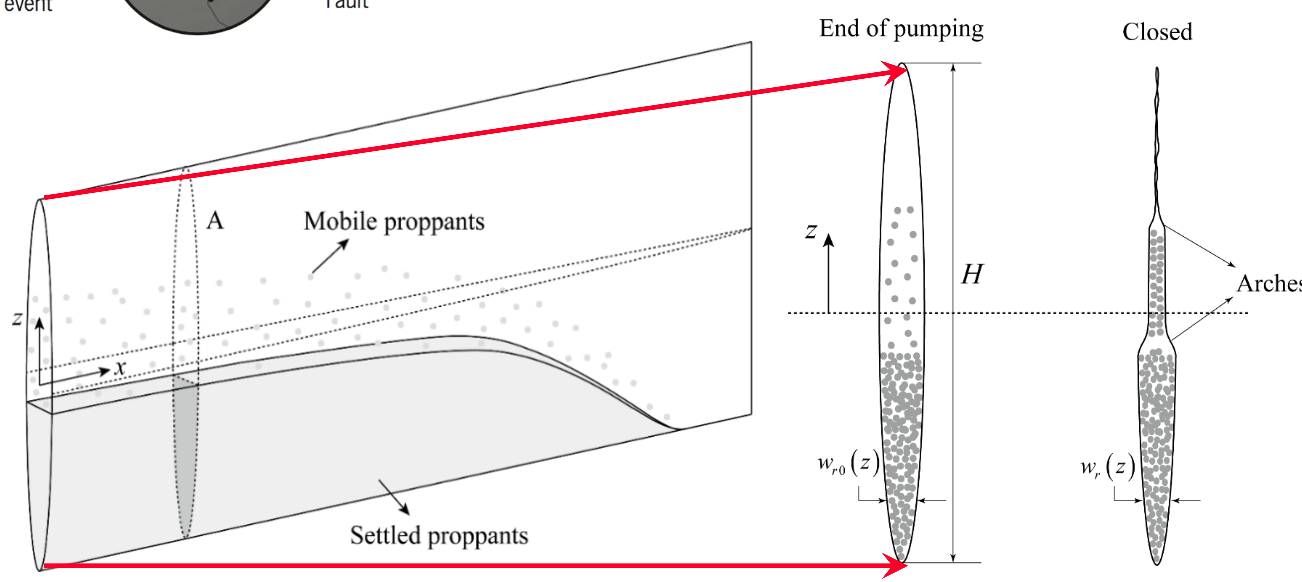

Propagation, Proppant Transport and the Evolution of Transport Properties of HFs

Propagation, Proppant Transport and the Evolution of Transport Properties of HFs

- Static Gas Fracturing
  - Rationale for Its Use
  - Physical Characteristics and Key Observations
  - Methods of Analysis
  - Unresolved Issues
- **Key Connections to Dynamic Gas Fracturing**
  - **Key observations**
  - **Essence of Dynamic Response**
  - **Zeroth- and First-Order Models**
- Proppant Transport in Gas Fractured HFs (Jiehao Wang)
  - Deformation-Transport-Closure Models
  - Observations
- Evolution of Permeability in HFs (Jiehao Wang)
  - Closure-Compaction and Arching
  - Productivity Controls
- Microbially Enhanced CBM (Sheng Zhi)
- Summary


Huainan Coal Company, Huainan
1MW Coal-gas drainage generator
On 5%-30% CH_4
保 障 供

HPU Dynamic Gas (CO_2) Fracturing

Pressure rise-time

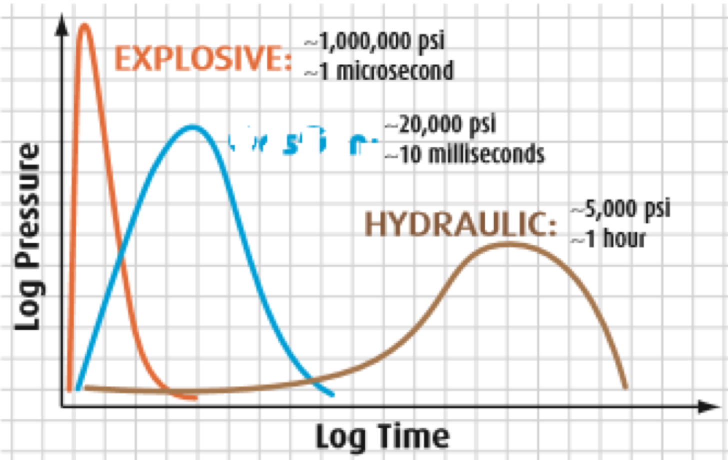

Pulverizing of coal

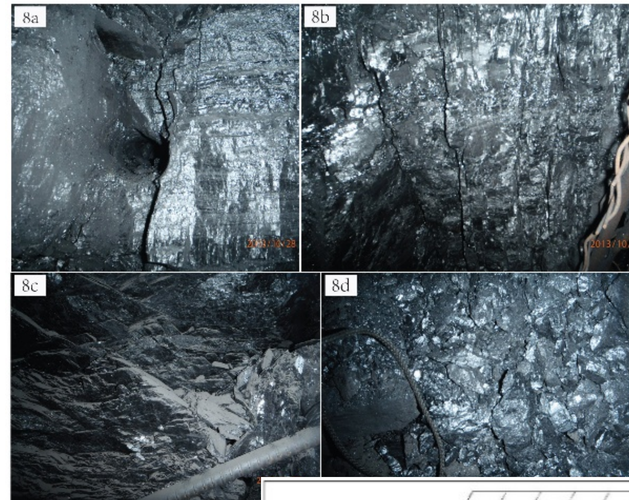

Damage zones

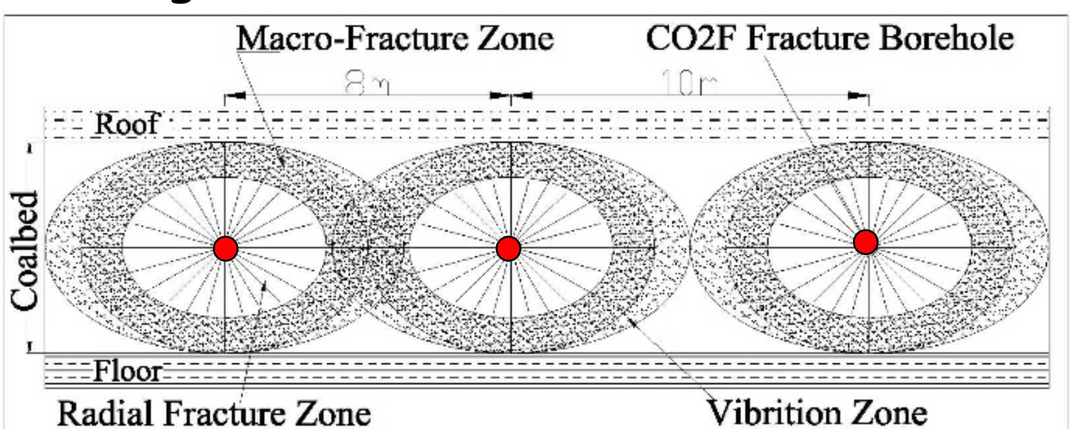

Radial fracturing

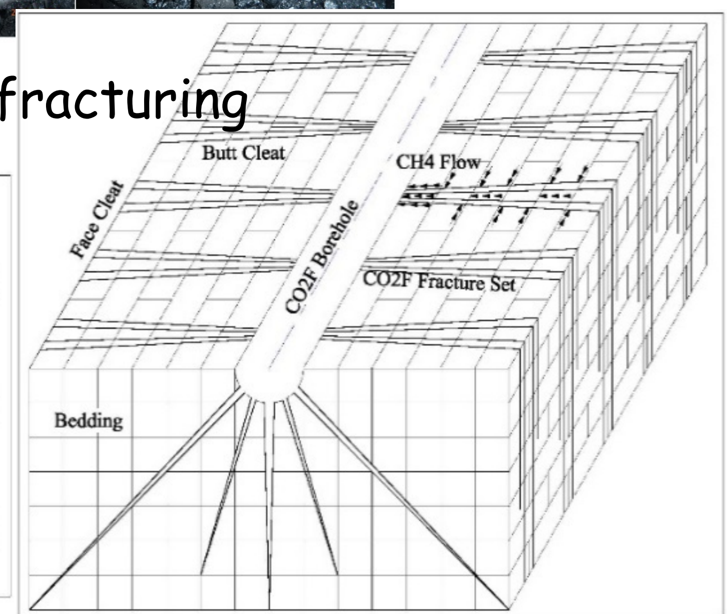

[Courtesy Yunxing Cao et al., HPU]

Controlling Influence of In Situ Stresses

Require to overcome static stresses to create a radial fracture network

Confining stress ratio of 6:1

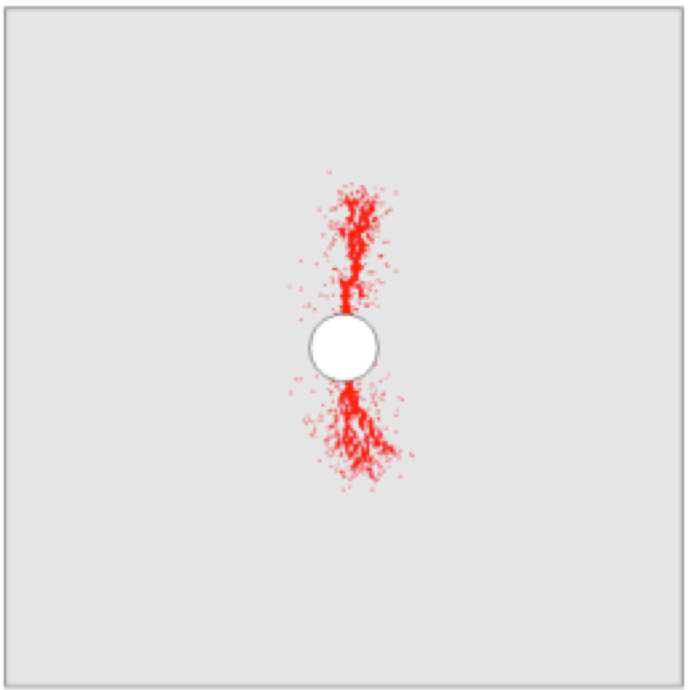

Confining stress ratio of 1:1

Dynamic Models

Field Equations

$$Gu_{i,jj} + \frac{G}{1-2\nu} u_{j,ji} + \alpha p_{,i} + F_i = \boxed{\rho_s \frac{\partial^2 u_i}{\partial t^2},}$$

$$\phi \frac{\partial p}{\partial t} - \nabla \cdot \left(\frac{k}{\mu} p \nabla p \right) = \frac{p_a}{\rho_{ga}} Q_s$$

Damage Mechanics Models

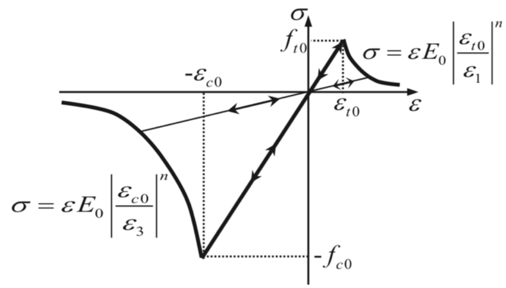

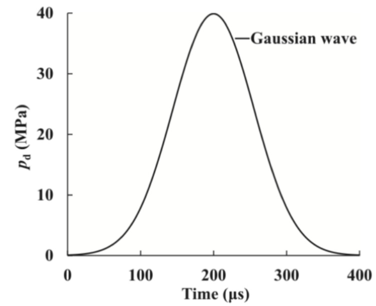

Dynamic Rupture

(a) Concrete specimen before blasting

(b) Front view after blasting

(c) Back view after blasting

Experimental Conditions

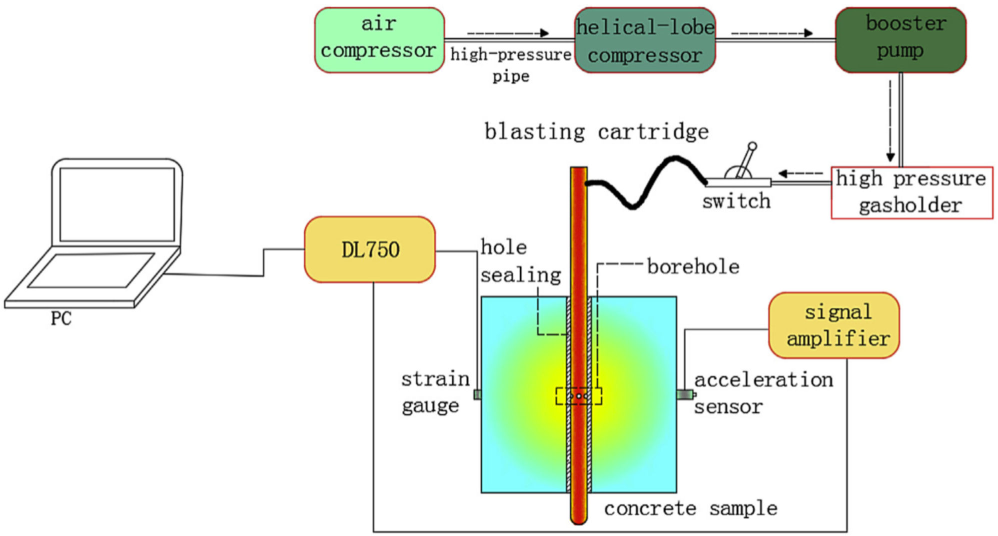

[Zhu et al., 2016]

Dynamic Stress Field

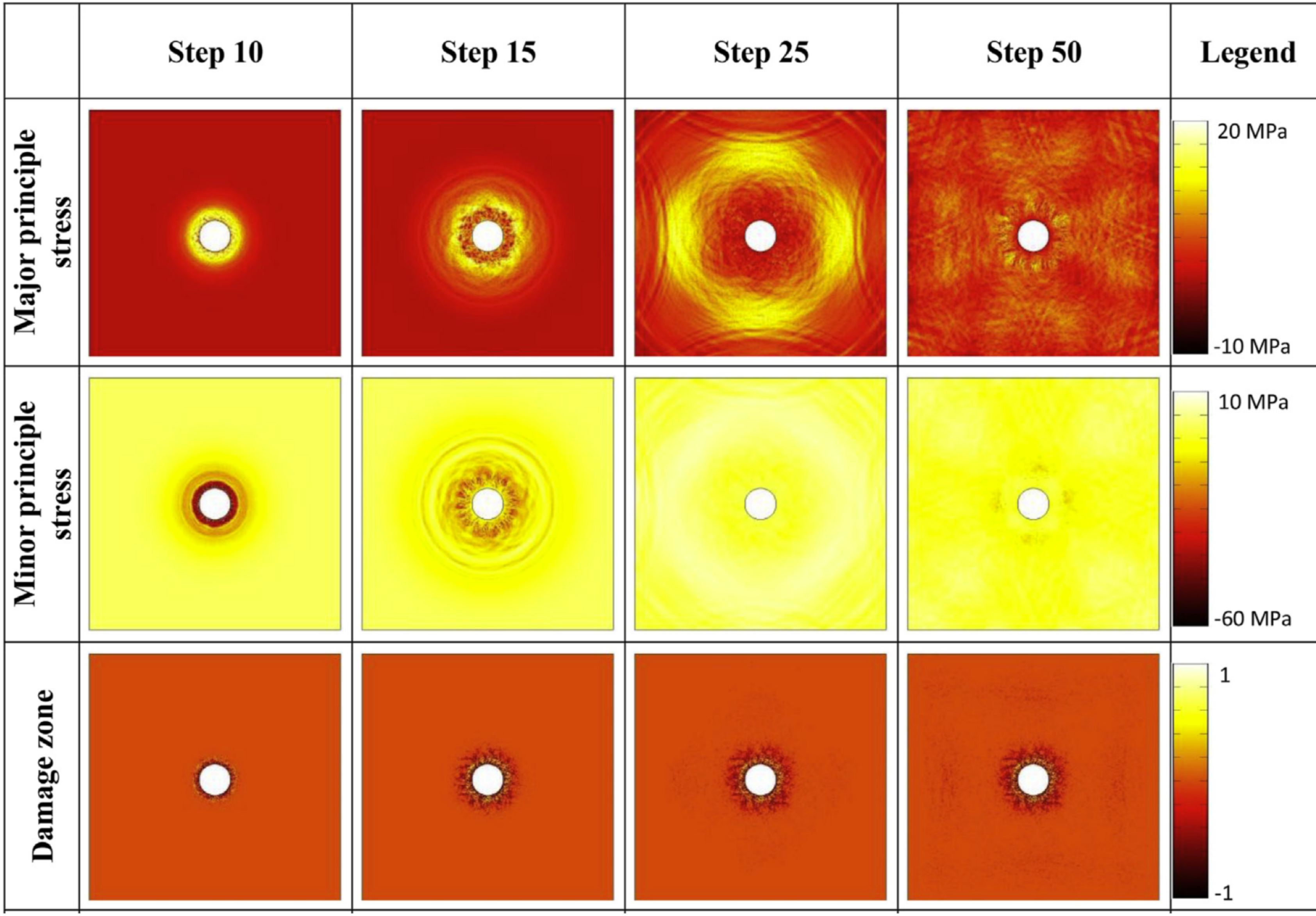

Damage Evolution

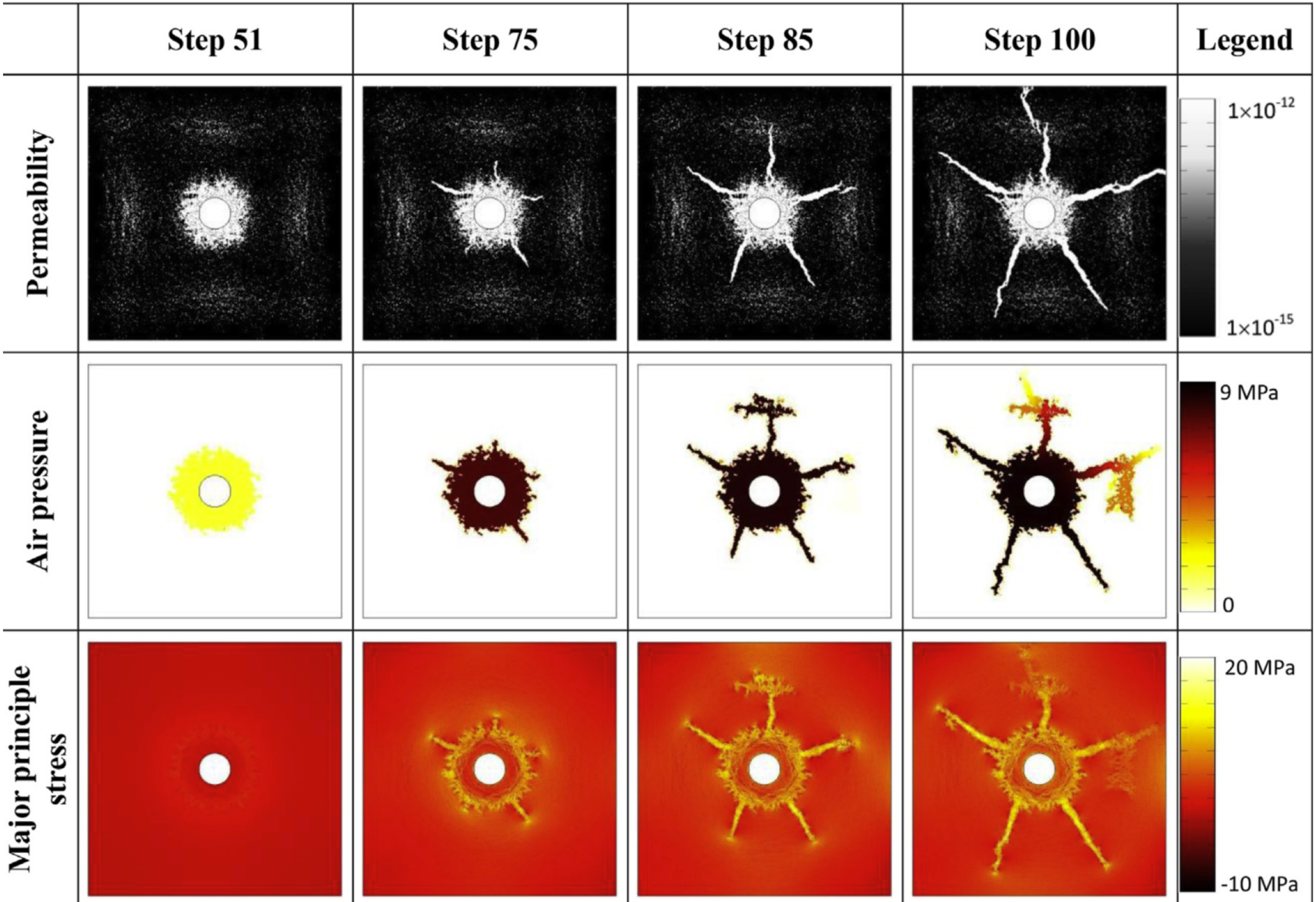

Impact of Pre-Existing Stress Field

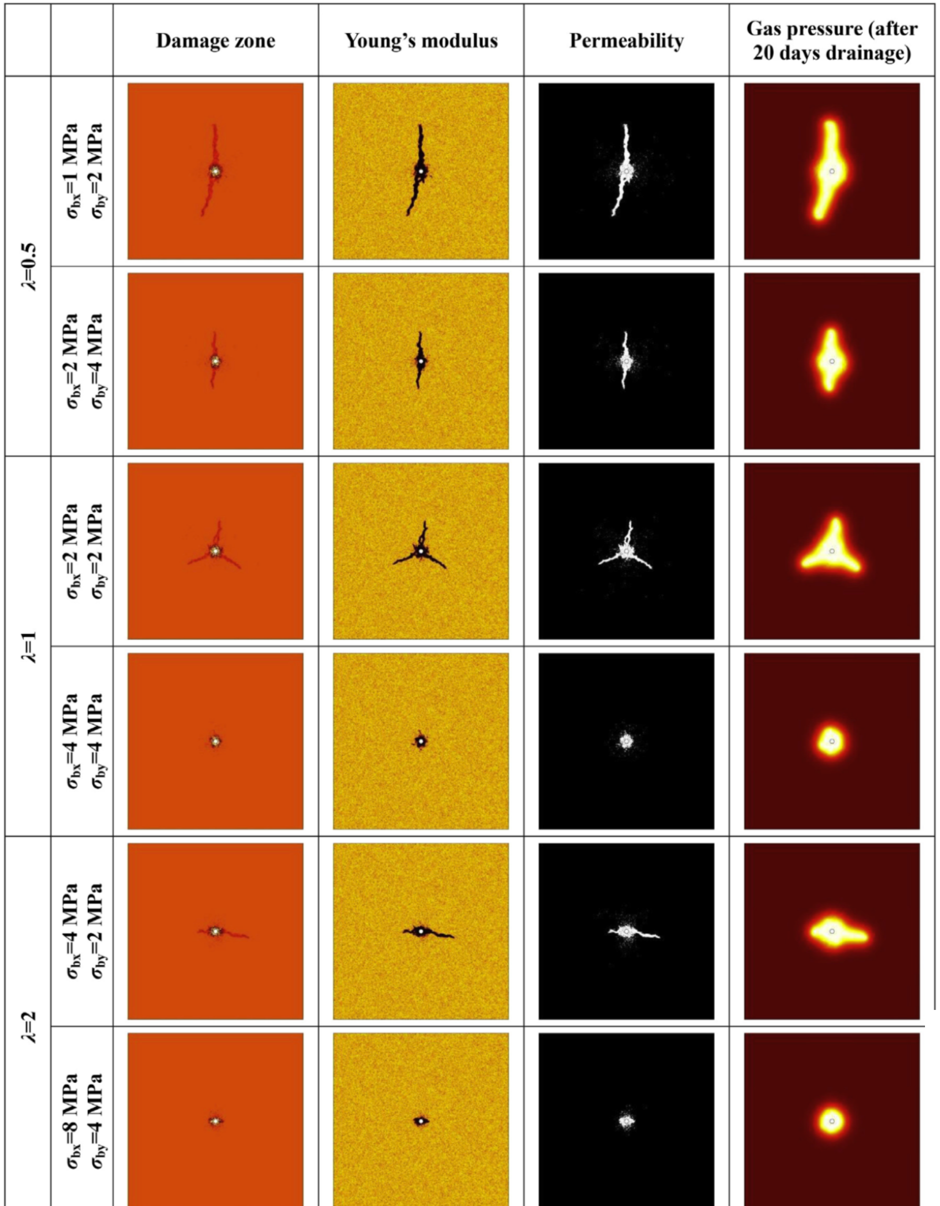

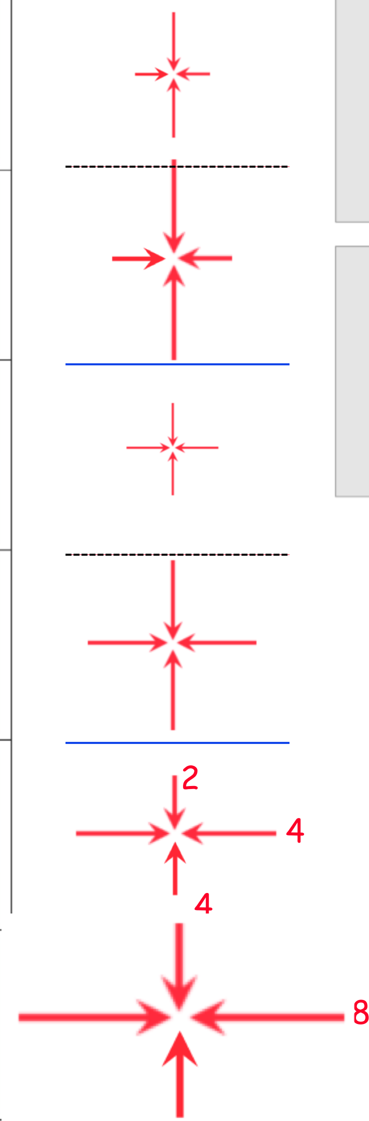

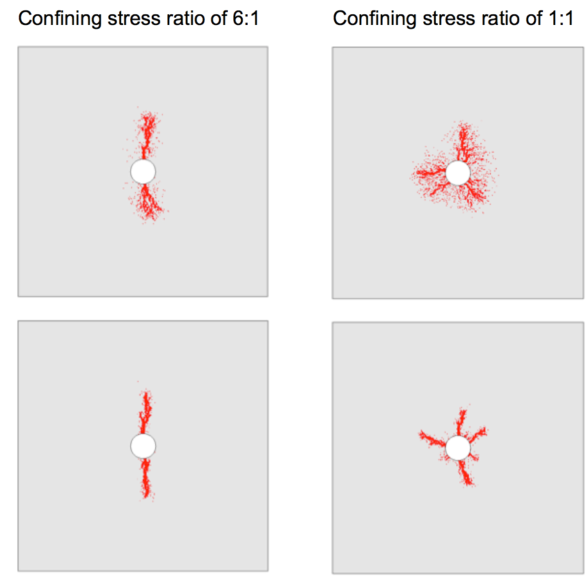

Propagation, Proppant Transport and the Evolution of Transport Properties of HFs

Problem Description and Assumptions

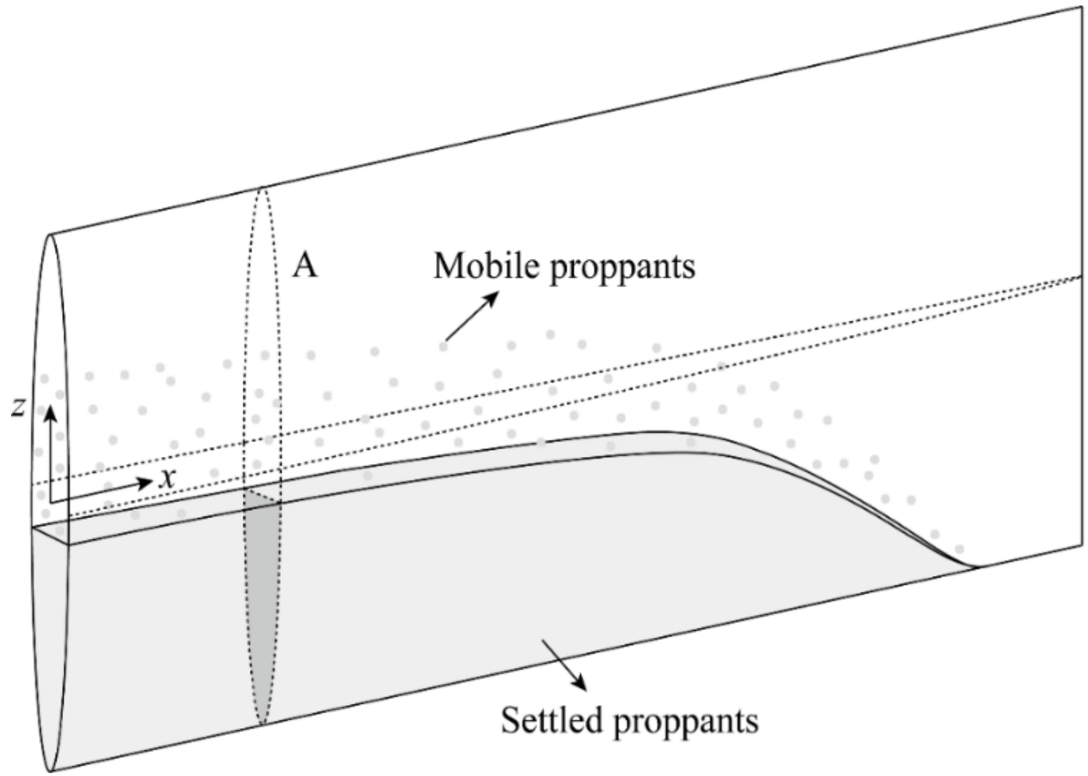

- Vertical fracture with a constant height and an elliptical cross-section.
- Plain strain in planes perpendicular to the propagation direction.
- Fluid pressure is assumed to be uniform over the height of the fracture.
- Fluid is Newtonian.
- Proppant particles are spheres with the same radius.
- Both proppant and fluid are incompressible.

Mathematical Formulation

(1) Fracture propagation (based on the PKN-formulism)

- Slurry Mass Balance

$$\frac{\partial \bar{w}(x,t)}{\partial t}+\frac{\partial \bar{q}^{s}(x,t)}{\partial x}+\frac{2C_l}{\sqrt{t-\tau(x)}}=0$$

- Width-pressure relationship

$$w(x,z,t)=\frac{2}{E'}\left(H^2-4z^2\right)^{1/2}p(x,t)$$

- Poiseuille's law

$$q^{s}(x,z,t)=-\frac{w^3(x,z,t)}{12\mu_f}\hat{Q}^{s}\left[\bar{\phi}(x,z,t),\frac{w(x,z,t)}{a}\right]\frac{\partial p(x,t)}{\partial x}$$

- Boundary conditions:

$$\bar{q}^{s}(0,t)=Q_0/2H \qquad \bar{w}(l,t)=0$$

- Initial condition: small time asymptotic solution.

$$\hat{Q}^{s}\left(\bar{\phi},\frac{w}{a}\right)=Q^{s}(\bar{\phi})+\frac{a^2}{w^2}\bar{\phi}D$$

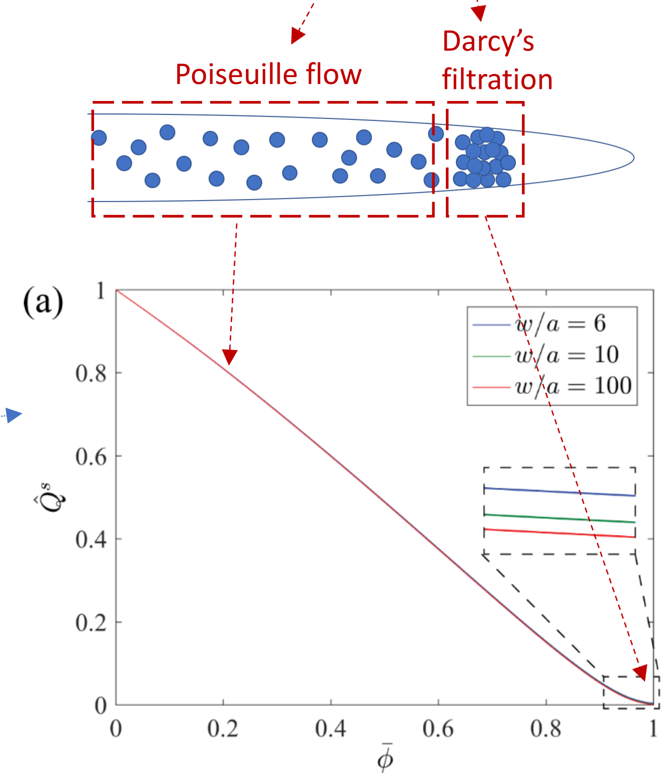

(Dontsov & Peirce, 2014)

Mathematical Formulation

(2) Proppant transport

- Proppant Mass Balance

$$\frac{\partial w(x,z,t)\bar{\phi}(x,z,t)}{\partial t}+\frac{\partial q_x^p(x,z,t)}{\partial x}+\frac{\partial q_z^p(x,z,t)}{\partial z}=0$$

- Proppant fluxes

$$q_x^p = B\left(\frac{w}{a}\right)\boxed{\hat{Q}^p\left(\bar{\phi},\frac{w}{a}\right)}q^s$$

$$q_z^p = -\boxed{B\left(\frac{w}{a}\right)}\frac{a^2 w}{12\mu_f}\left(\rho_p-\rho_f\right)g\boxed{\hat{G}^p\left(\bar{\phi},\frac{w}{a}\right)}$$

Blocking function

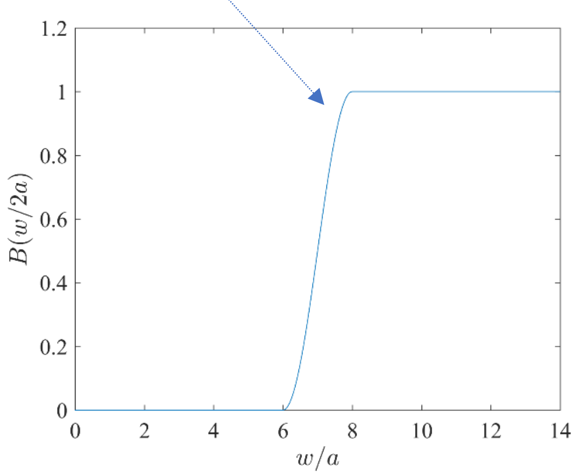

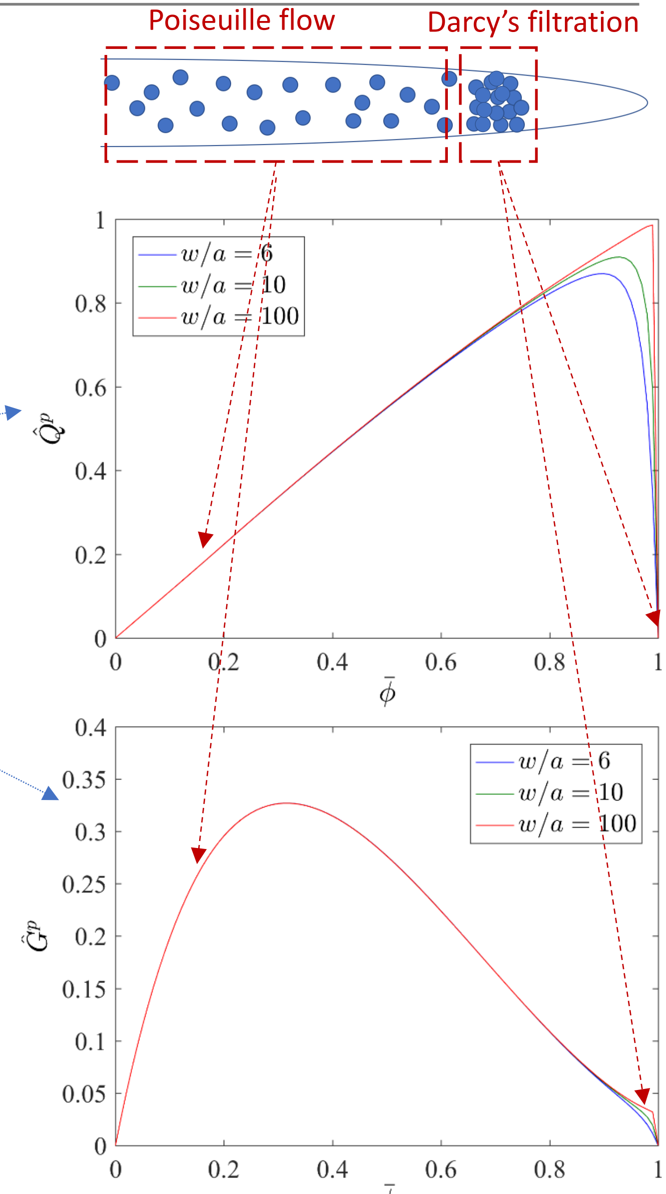

(Dontsov & Peirce, 2014)

Numerical Algorithm

- Moving coordinate

$$0 \le x \le l(t) \quad \Rightarrow \quad \xi = \frac{x}{l(t)}, \quad 0 \le \xi \le 1$$

- Transformations of spatial and time derivatives

$$\left.\frac{\partial(\cdot)}{\partial t}\right|_x = \left.\frac{\partial(\cdot)}{\partial t}\right|_\xi - \xi \frac{\dot{l}}{l} \left.\frac{\partial(\cdot)}{\partial \xi}\right|_t \qquad \left.\frac{\partial(\cdot)}{\partial x}\right|_t = \frac{1}{l} \left.\frac{\partial(\cdot)}{\partial \xi}\right|_t$$

- Governing equations under the moving coordinate

Update fracture length and width, and slurry flux

- Fracture propagation

$$\frac{\partial \overline{w}}{\partial t} - \xi \frac{\dot{l}}{l} \frac{\partial \overline{w}}{\partial \xi} + \frac{1}{l} \frac{\partial \overline{q}^s}{\partial \xi} + \frac{2C_l}{\sqrt{t - \tau(l\xi)}} = 0$$

(Solved by a collocation scheme)

- Proppant transport

$$\frac{\partial w\overline{\phi}}{\partial t} + \frac{\dot{l}}{l} w\overline{\phi} + \frac{1}{l} \frac{\partial \tilde{q}_x^p}{\partial \xi} + \frac{\partial q_z^p}{\partial z} = 0$$

(Solved by a finite volume method)

Update proppant distribution

Results: water

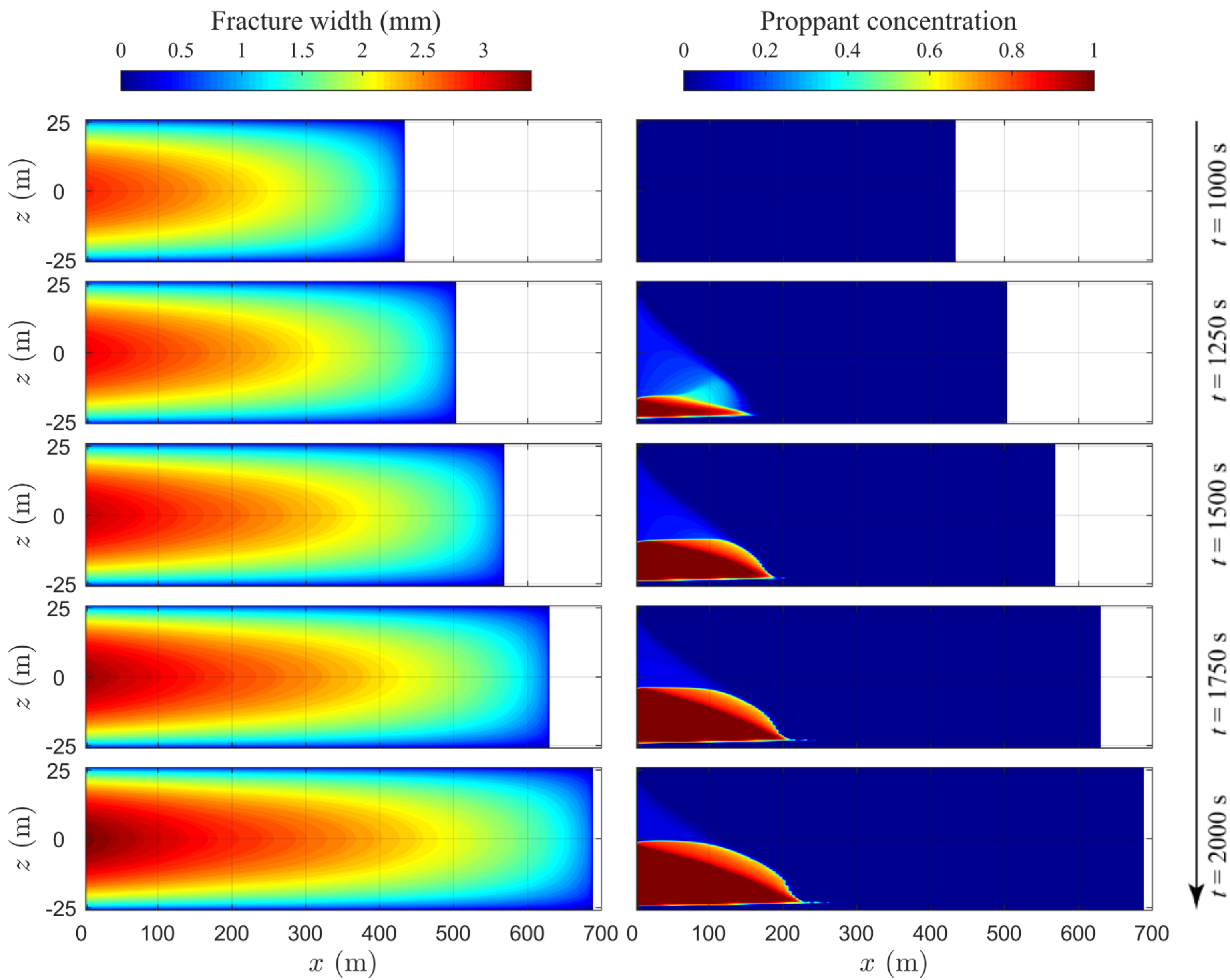

Results: LPG

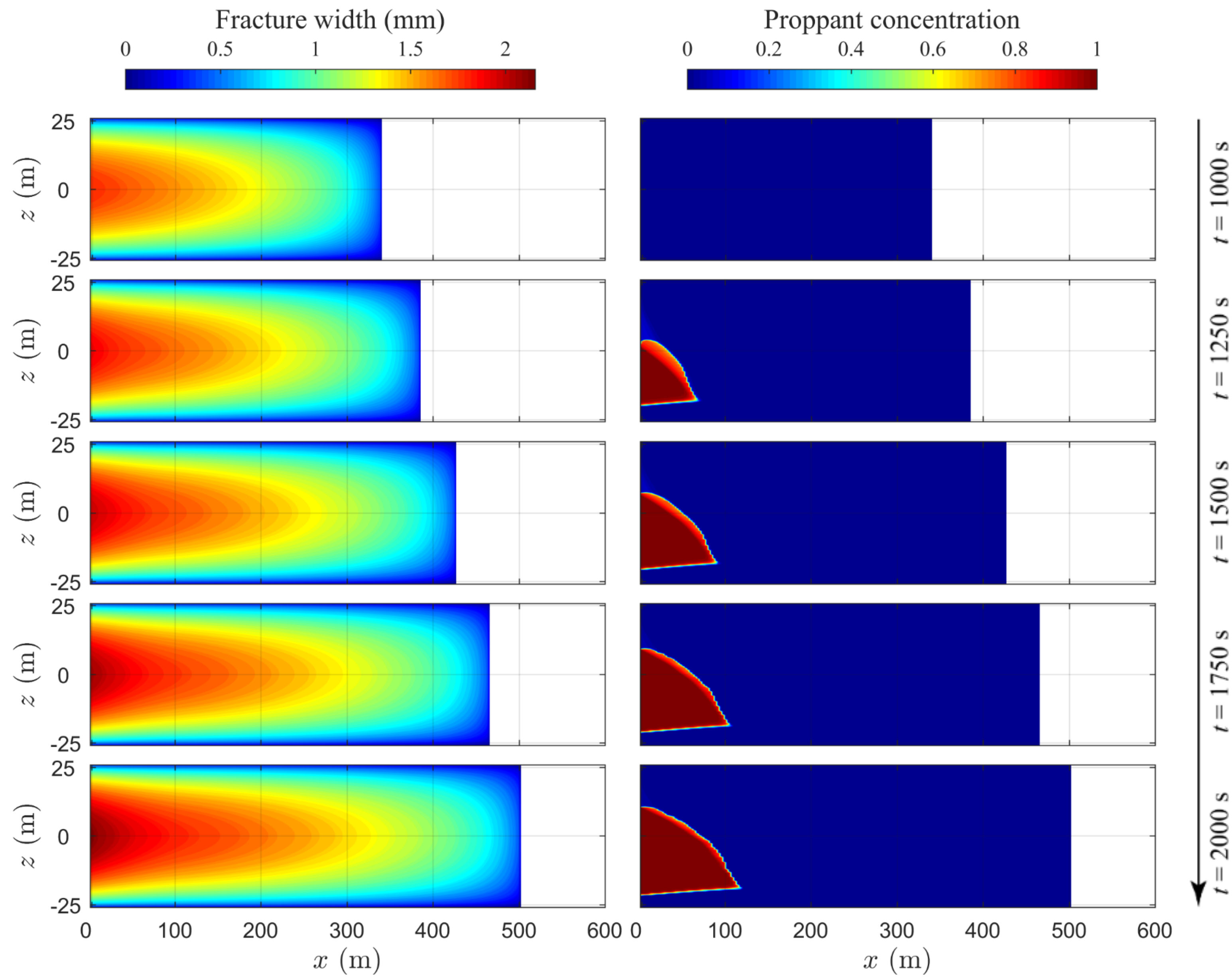

Fracture width (mm)
0
0.5
1
1.5
2
Proppant concentration
0
0.2
0.4
0.6
0.8
1
25
0
-25
z (m)
0
100
200
300
400
500
600
x (m)
t = 1000 s
t = 1250 s
t = 1500 s
t = 1750 s
t = 2000 s

Results: CO_2

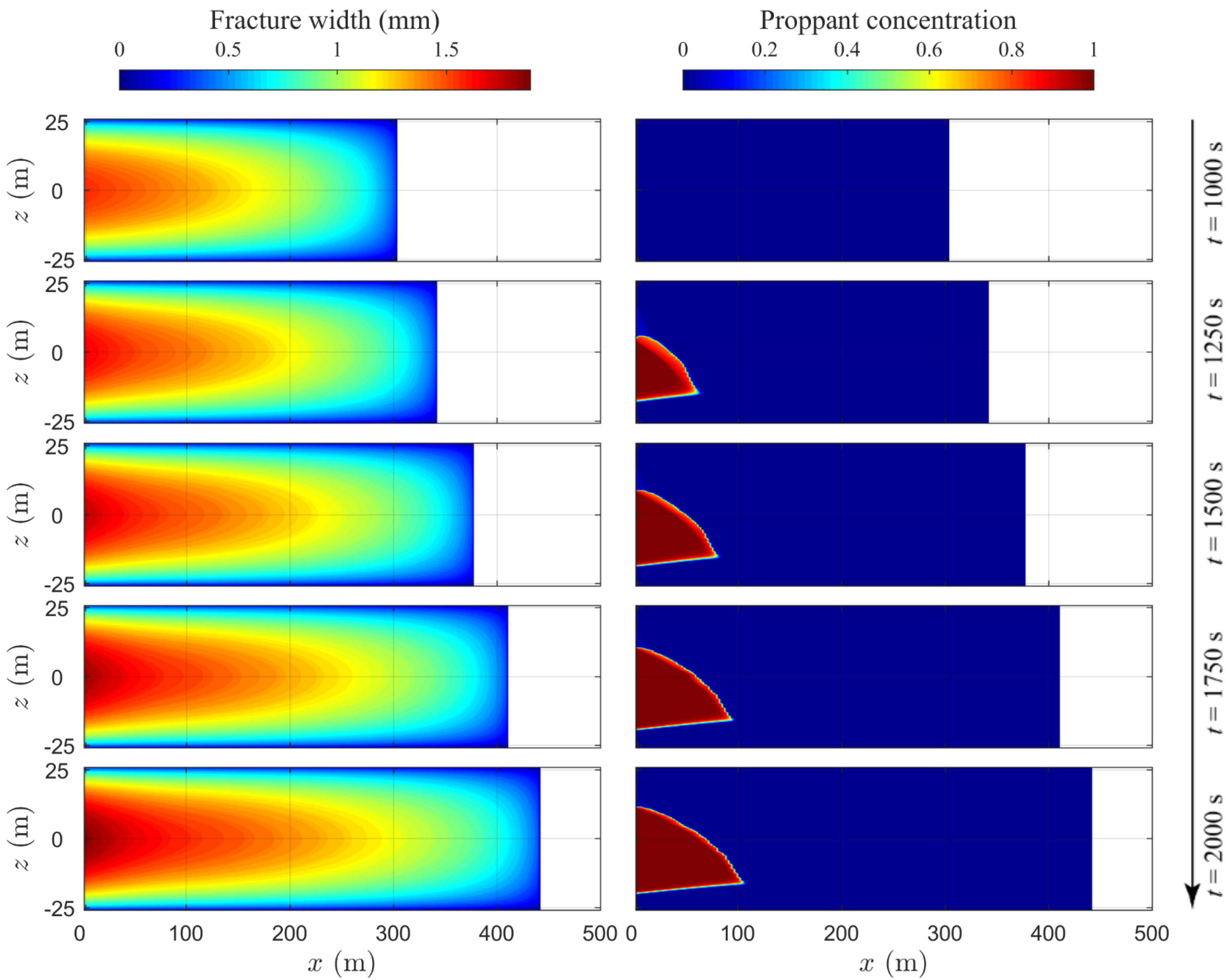

Fracture width (mm)
0
0.5
1
1.5
Proppant concentration
0
0.2
0.4
0.6
0.8
1
25
0
-25
z (m)
0
100
200
300
400
500
x (m)
t = 1000 s
t = 1250 s
t = 1500 s
t = 1750 s
t = 2000 s

Results: ethane

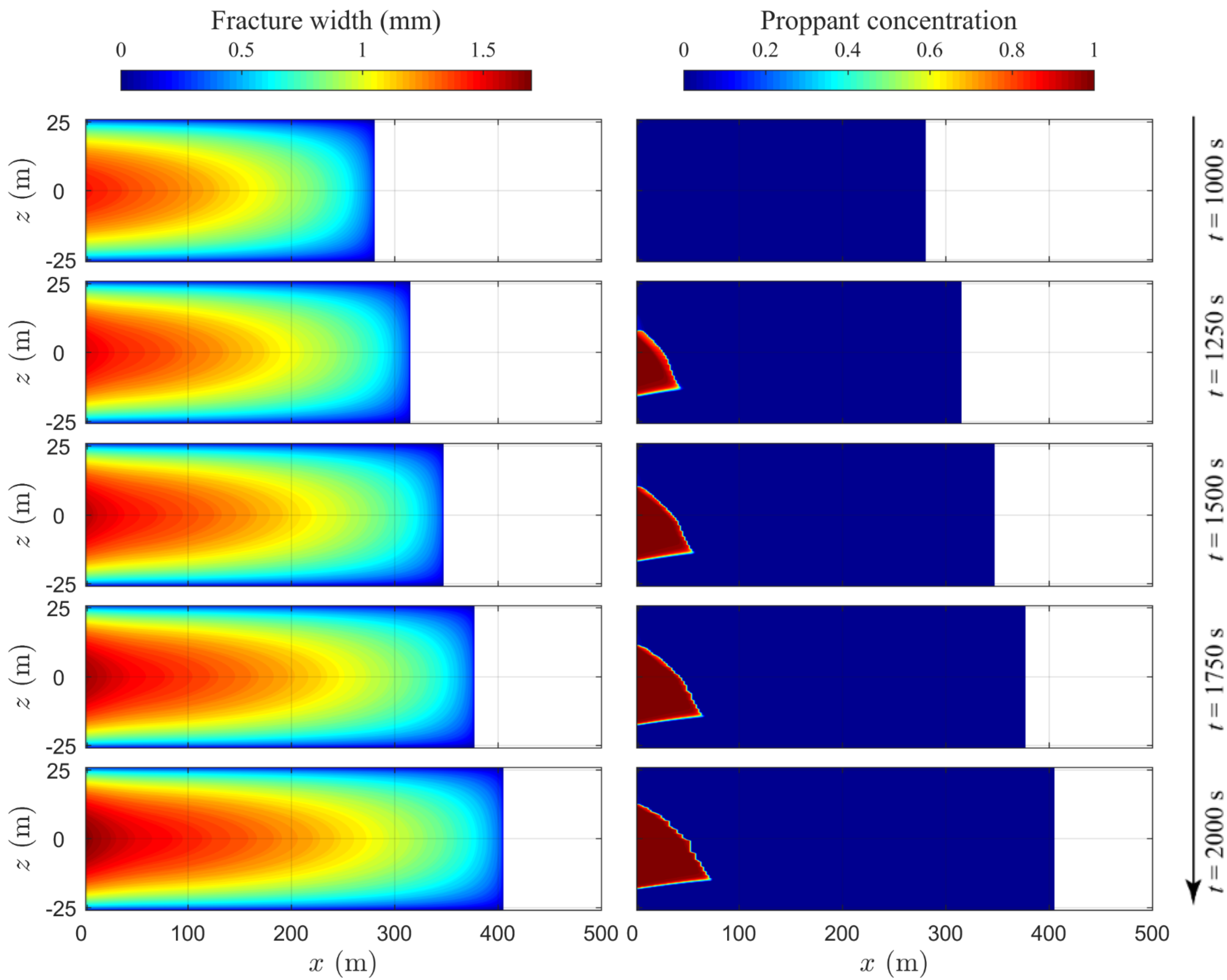

Results: N_2

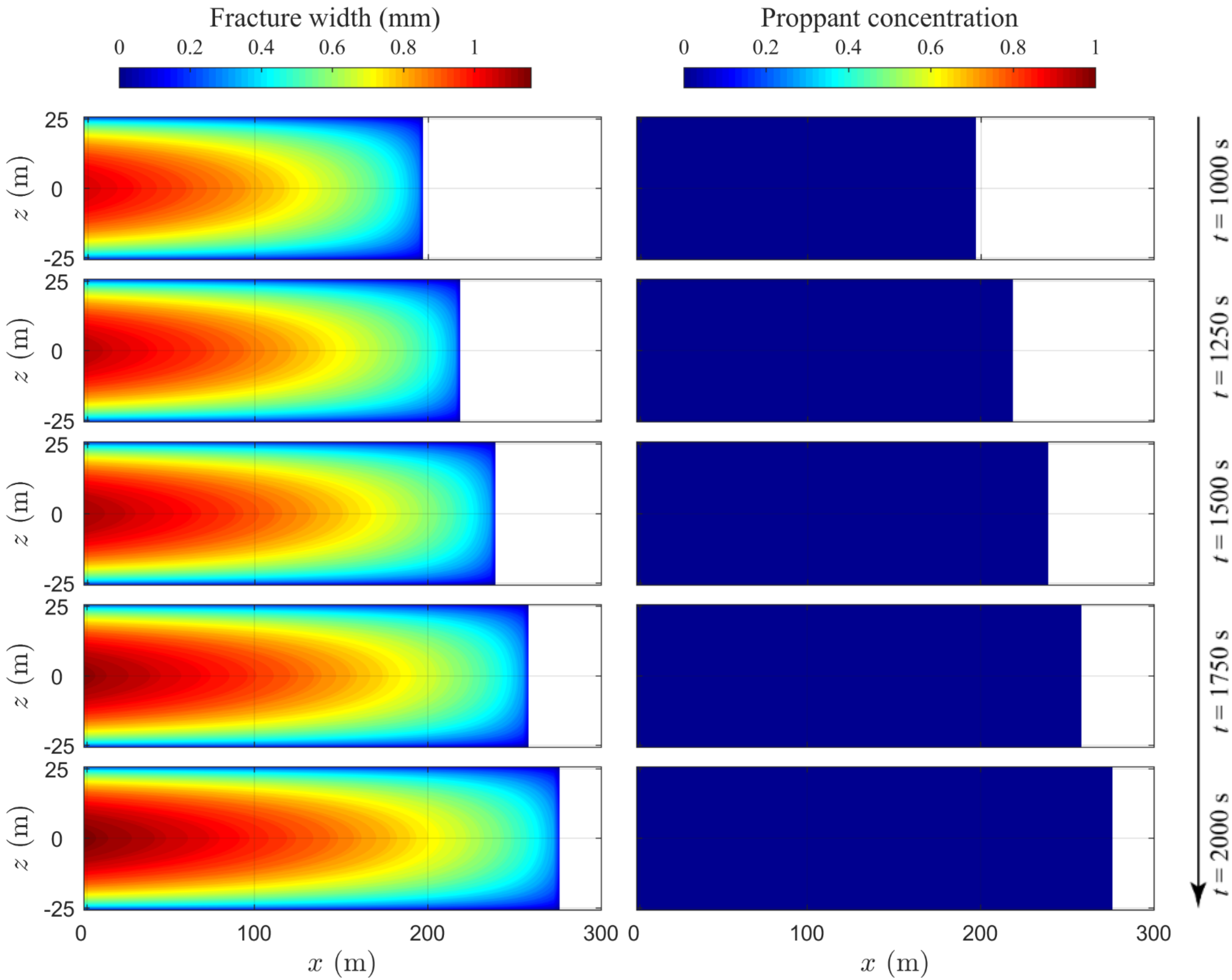
Fracture width (mm)
0 0.2 0.4 0.6 0.8 1
Proppant concentration
0 0.2 0.4 0.6 0.8 1
25
0
-25
z (m)
0 100 200 300
x (m)
t = 1000 s
t = 1250 s
t = 1500 s
t = 1750 s
t = 2000 s

Results

Fracture profile

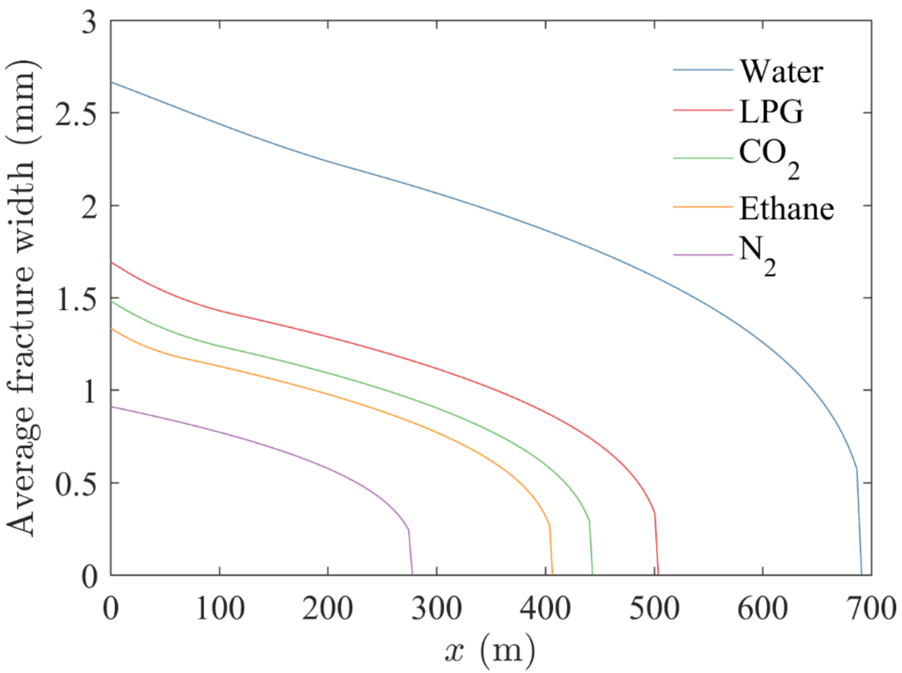

Proppant distribution

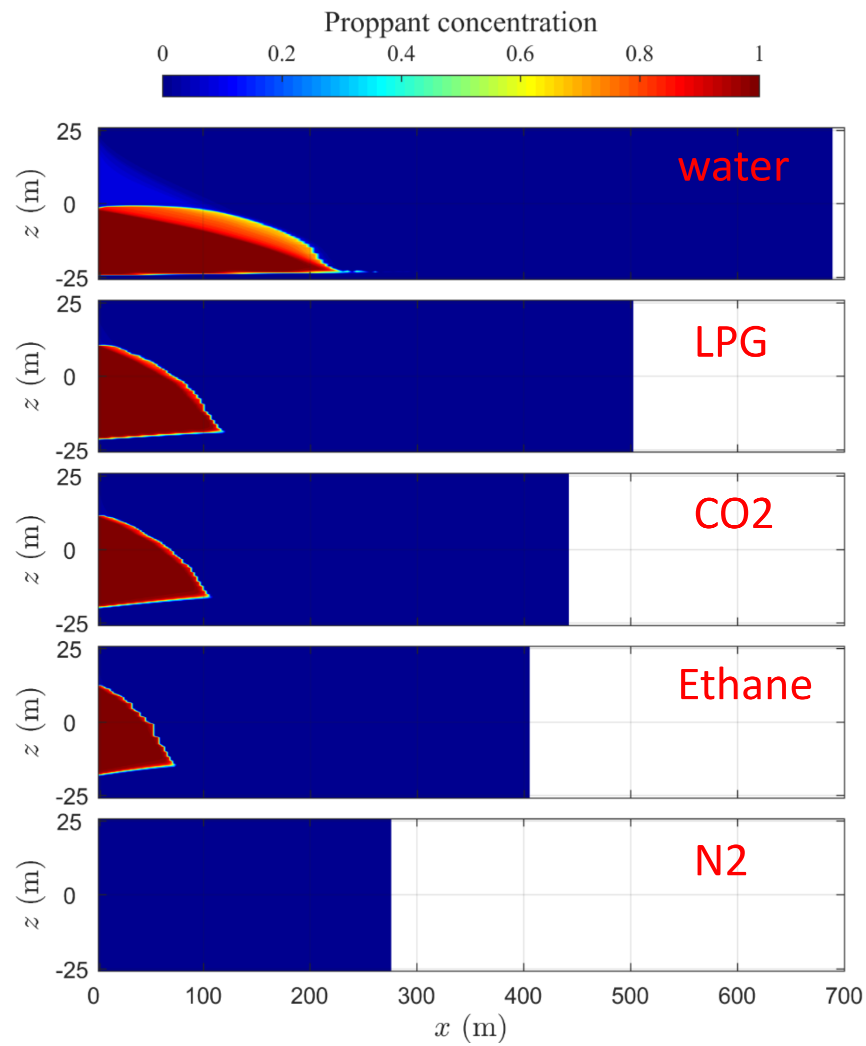

How to improve proppant infusion length?

Ultra-light weight proppant

- rho_proppant=1050 kg/m^3
- Ethane

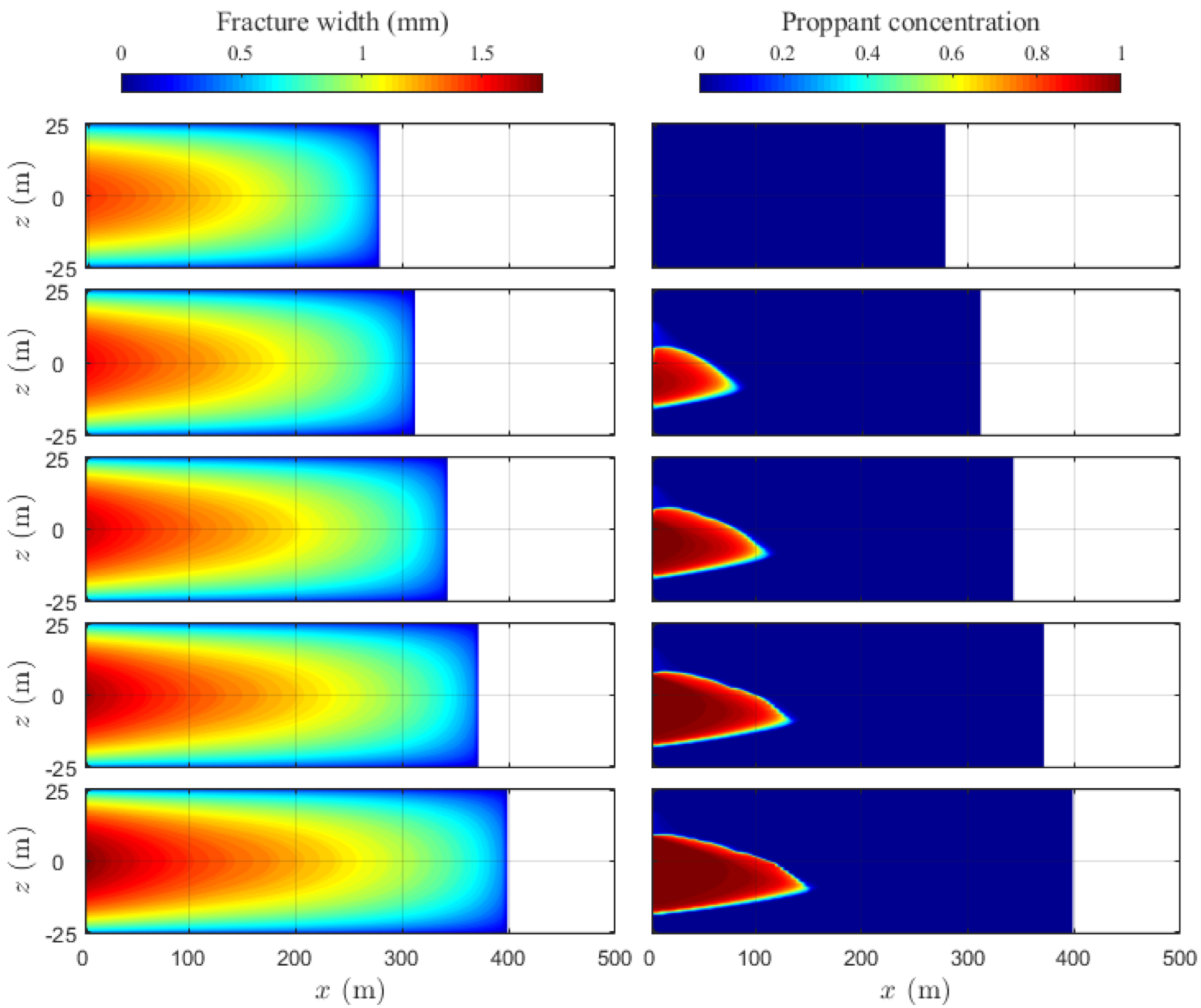

Analysis

Horizontal velocity of proppant

$$\bar{w}_w = \left(\frac{\pi\mu Q_0}{E'C_l H}\right)^{1/4} t^{1/8}$$

Leakoff-dominated approximation

$$q^s = \frac{Q_0}{2H}$$

$$t = \frac{t_{inj} + t_{end}}{2}$$

$$\bar{v}_x^p = \frac{Q_0}{2H\bar{w}_w}\cdot\frac{6}{5} = \frac{3}{5}\left(\frac{E'C_l Q_0^2}{\pi\mu H^3}\right)^{1/4}\left(\frac{1}{t}\right)^{1/8}$$

Settling time

$$v_z^p = \frac{a^2\left(\rho_p - \rho_f\right)g}{12\mu}\cdot\frac{8}{3} = \frac{2a^2\left(\rho_p - \rho_f\right)g}{9\mu}$$

$$t_s = \frac{H}{v_z^p} = \frac{9H\mu}{2a^2\left(\rho_p - \rho_f\right)g}$$

Length of proppant bank

$$C_l = \sqrt{\frac{kn\Delta p}{2\mu}}$$

$$L = \bar{v}_x^p t_s = \frac{3}{5}\left(\frac{E'C_l Q_0^2}{\pi\mu H^3}\right)^{1/4}\left(\frac{1}{t}\right)^{1/8}\frac{9H\mu}{2a^2\left(\rho_p - \rho_f\right)g} = \frac{27}{10g}\left(\frac{E'Q_0^2 H}{\pi}\right)^{1/4}\left(\frac{kn\Delta p}{2t}\right)^{1/8}\boxed{\frac{\mu^{5/8}}{a^2\left(\rho_p - \rho_f\right)}}$$

Term related with properties of fracturing fluid and proppant

Analysis

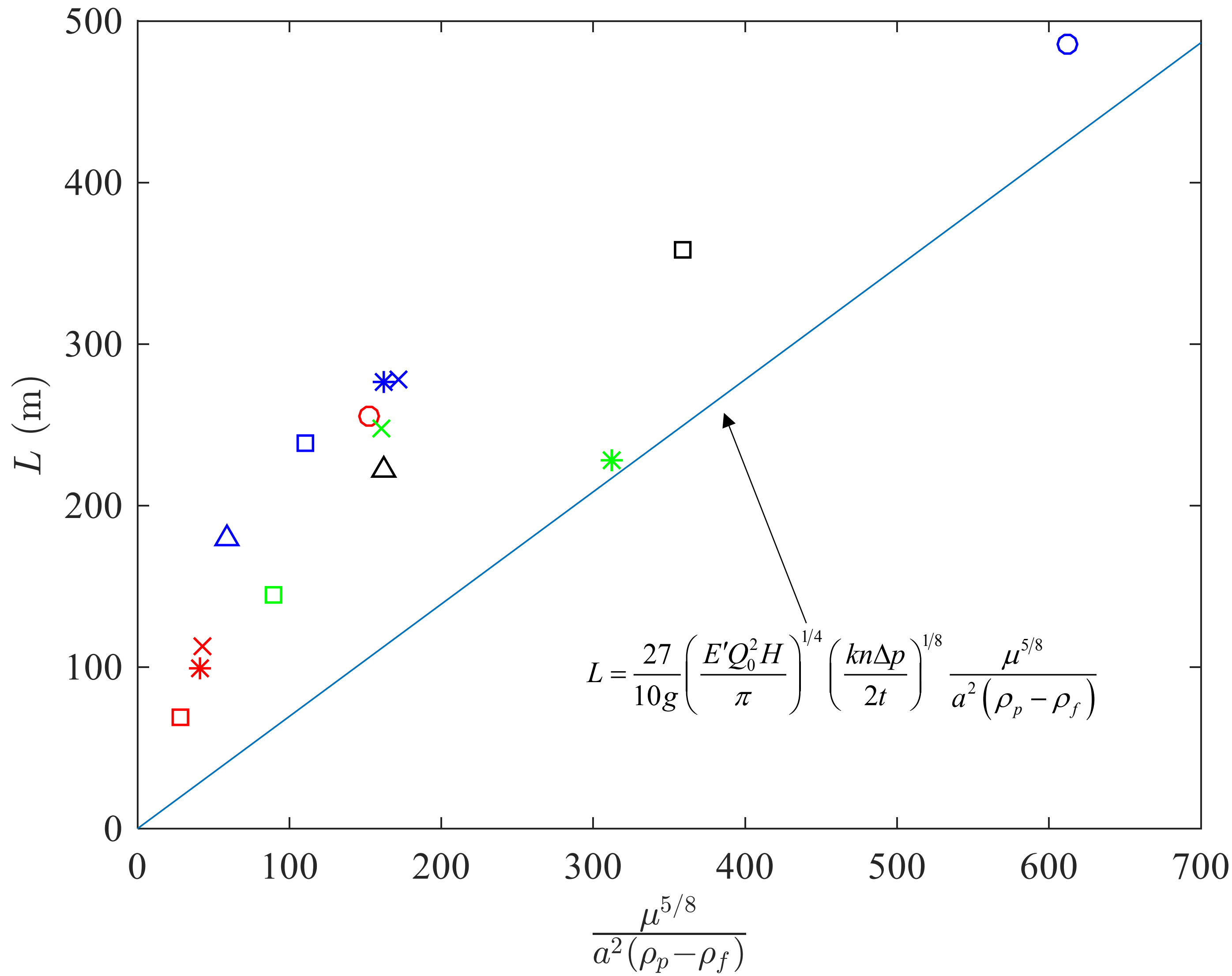

Shape

- △ N_2
- □ Ethane
- ✱ CO_2
- × Propane
- ○ Water

Color

Red: standard cases

Blue: small size proppant

Green: light weight proppant

Black: small size + light weight

Propagation, Proppant Transport and the Evolution of Transport Properties of HFs

Static Gas Fracturing
- Rationale for Its Use
- Physical Characteristics and Key Observations
- Methods of Analysis
- Unresolved Issues

Key Connections to Dynamic Gas Fracturing
- Key observations
- Essence of Dynamic Response
- Zeroth- and First-Order Models

Proppant Transport in Gas Fractured HFs (Jiehao Wang)
- Deformation-Transport-Closure Models
- Observations

Evolution of Permeability in HFs (Jiehao Wang)
- **Closure-Compaction and Arching**
- **Productivity Controls**

Microbially Enhanced CBM (Sheng Zhi)

Summary

Problem Description and Assumptions

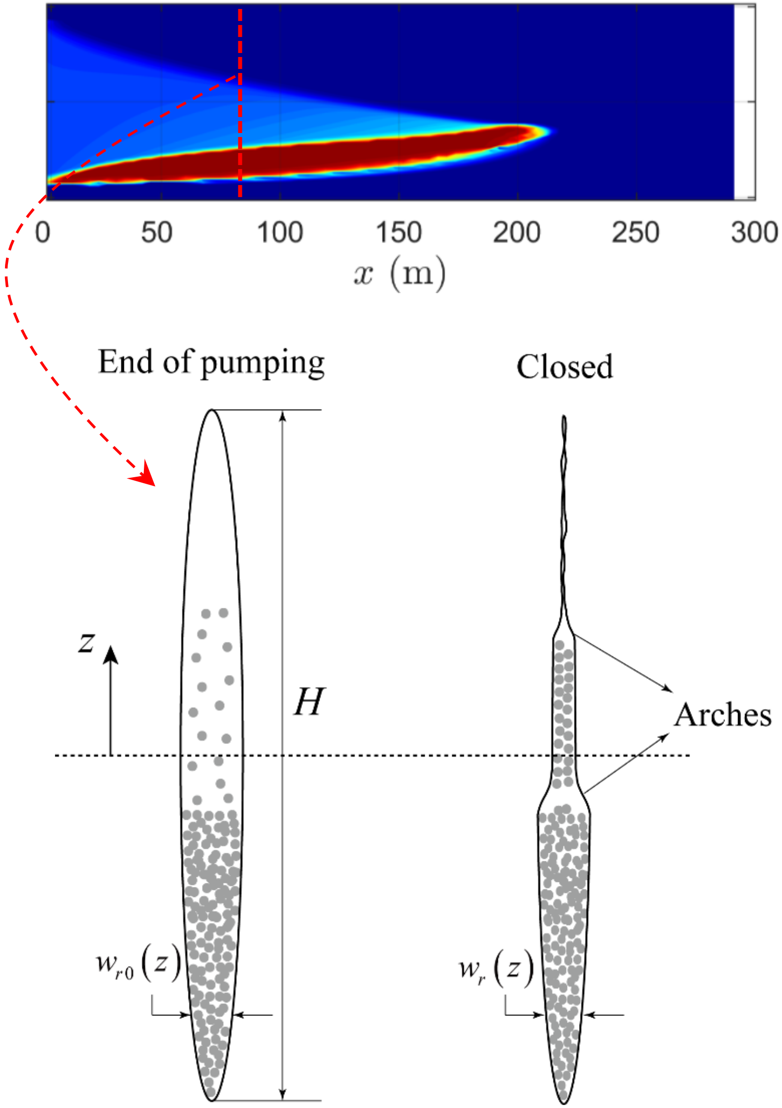

Given fracture geometry, proppant distribution, and fluid pressure;

Solve for fracture residual aperture profile and fracture conductivity.

Assumptions:

- Formation is linear elastic, isotropic, and homogenous.
- Plain strain in planes perpendicular to the *x* direction.
- Proppant particles are incompressible.
- Proppant packs have a constant compressibility.
- Proppant never crush.

Mathematical Formulation

(1) Elastic integral equation

$$w_r(x,z) = \frac{4}{\pi E'}\int_{-H/2}^{H/2} \sigma_n(x,s) G(z,s)\, ds - 2w_e(x,z)$$

Residual aperture (w_r)

Net normal stress on fracture walls (σ_n)

Proppant embedment (w_e)

where $G(z,s) = \cosh^{-1}\dfrac{H^2 - 4sz}{2H|z-s|}$

$$\sigma_n(x,z) = p_f(x,z) - \sigma_h + \sigma_p(x,z) + \sigma_a(x,z)$$

- *Fluid pressure* (p_f)
- *Minimum in-situ stress* (σ_h)
- *Stress applied by proppant pack* (σ_p)
- *Contact stress on the unpropped, closed span of the fracture* (σ_a)

Need to define: $\sigma_a \sim w_r$

$\sigma_p \sim w_r$

$w_e \sim w_r$

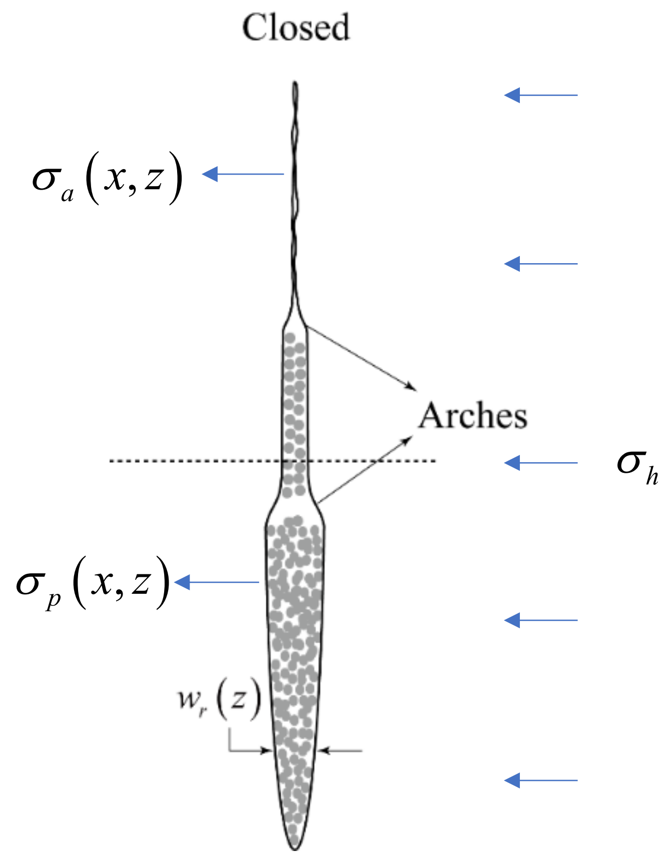

Mathematical Formulation

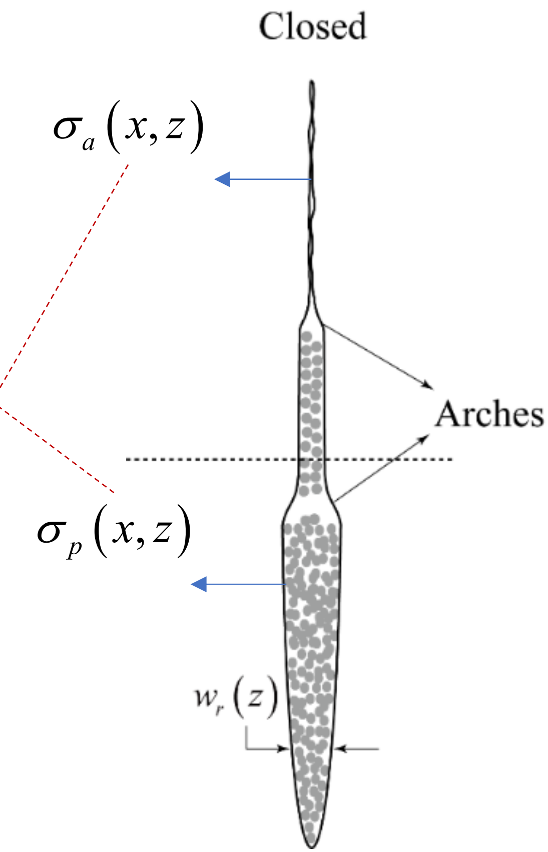

(2) Compaction of proppant pack (define)

By the definition of compressibility

$$\sigma_p(x,z) = \frac{1}{c_p} \ln \frac{w_{r0}(x,z)\bar{\phi}_{r0}(x,z)}{w_r(x,z)}$$

(3) Mechanical response of rough fracture (define)

Barton-Bandis fracture closure model

$$\sigma_a(x,z) = \frac{w_a - w_r(x,z)}{b_1 - b_2\left[w_a - w_r(x,z)\right]}$$

(Bandis et al., 1983; Barton et al., 1985)

(4) Proppant embedment (define)

By Hertzian contact theory

$$w_e(x,z) = a\left(\frac{3\pi}{4E'}\right)^2 \left[\frac{16\eta E'^2}{9\pi^3 c_p} \ln \frac{w_{r0}(x,z)\bar{\phi}_{r0}(x,z)}{w_r(x,z)}\right]^{2/3}$$

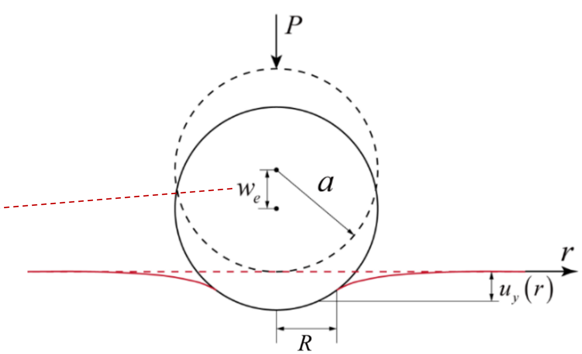

Numerical Results: 1D cases

Base case

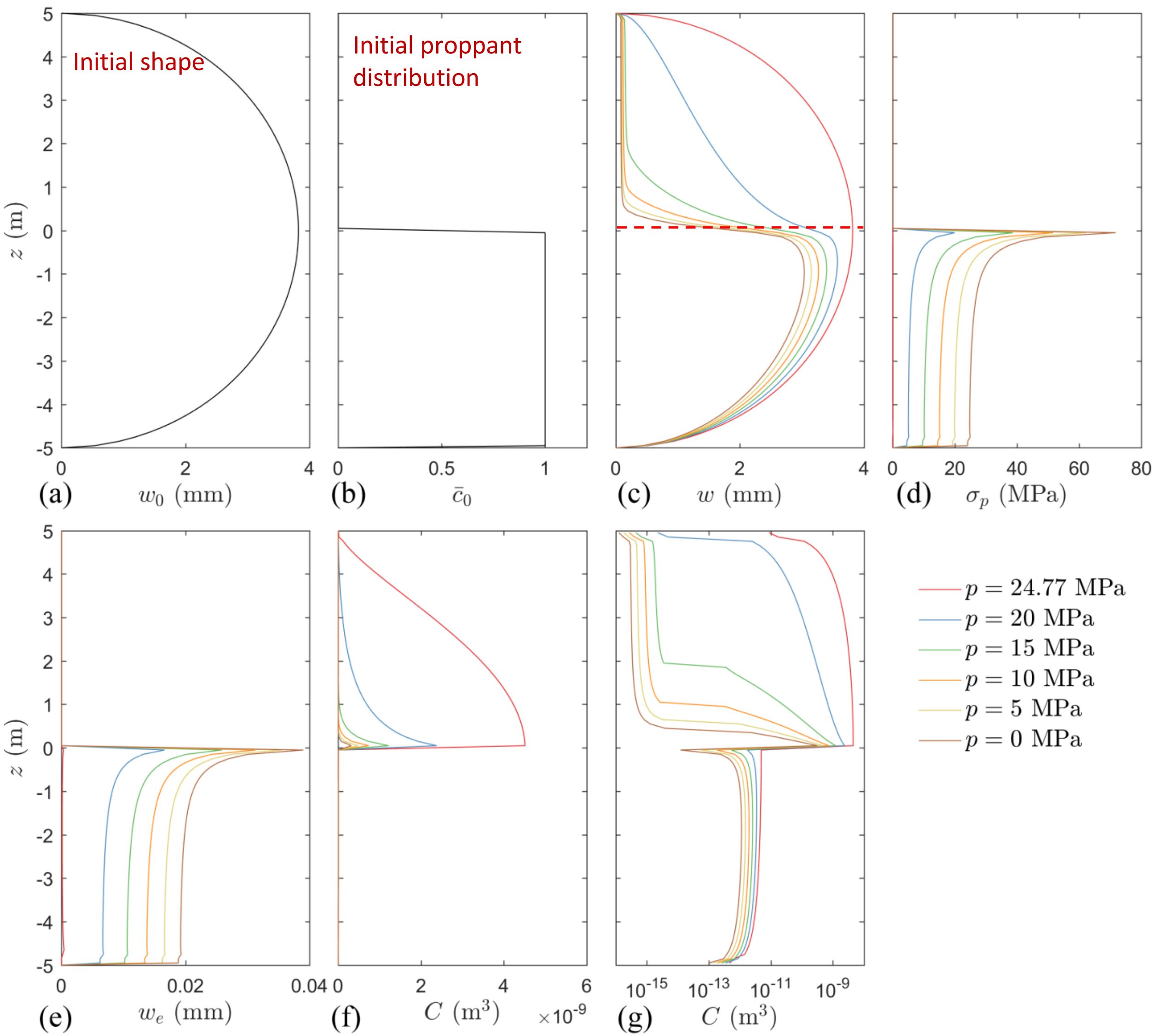

(a) Initial shape of the fracture; (b) initial distribution of the normalized proppant concentration; and the evolution of (c) fracture width, (d) compacting stress on proppant pack, (e) proppant embedment, and fracture conductivity (f) in natural scale and (g) in logarithmic scale as fluid pressure decreases.

Numerical Results: 1D cases

Effect of proppant bed height

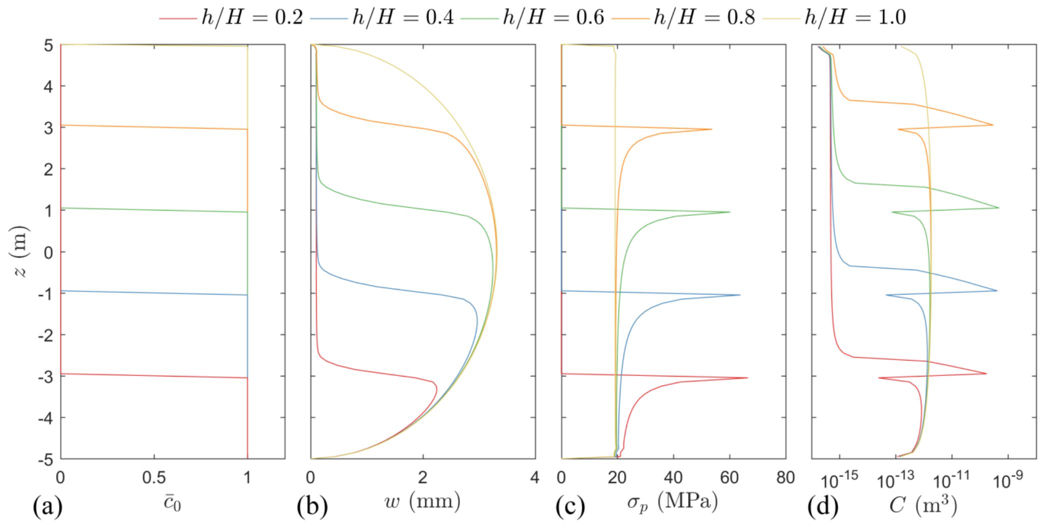

Effect of proppant bed width

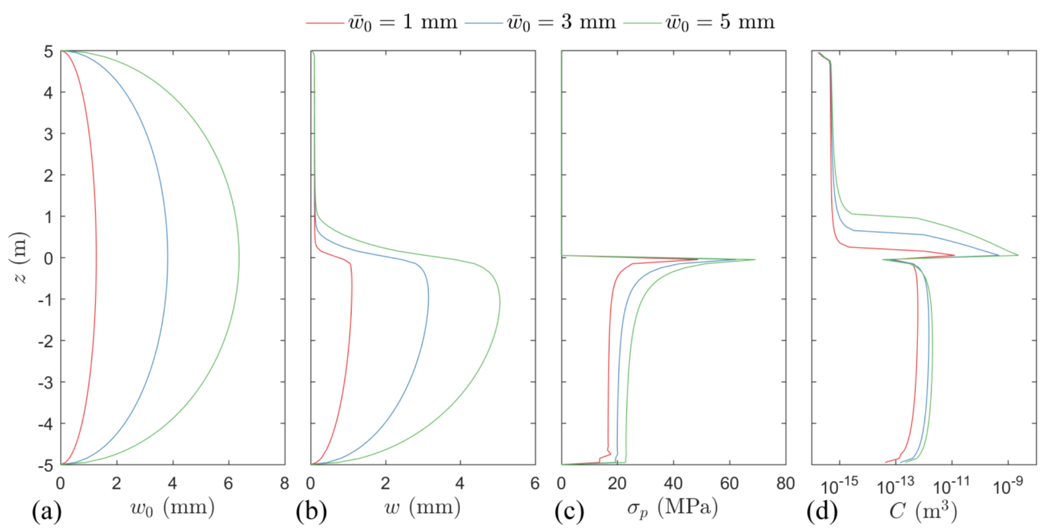

(a) initial proppant distributions;

(b) residual opening profiles;

(c) resultant compacting stresses applied on proppant bed;

(d) fracture conductivities after fracture closure.

Numerical Results: 2D cases

2D cases:

1) Base case;
2) Low fluid viscosity;
3) Large proppant size;
4) Small proppant density;
5) Fast leak-off rate;
6) Slick-water fracturing;

➢ Input parameters for the 2D cases

Parameters	Values
Minimum *in-situ* stress, σ_h	20 MPa
Fluid pressure within the fracture, p_f	10 MPa
Compressibility of proppant pack, c_p	7.25×10^{-9} Pa^{-1}
Asperity width, w_a	0.1 mm
Asperity compliance, b_1	1.43×10^{-11} Pa^{-1}

Numerical Results: 2D cases

(2) Low Fluid Viscosity

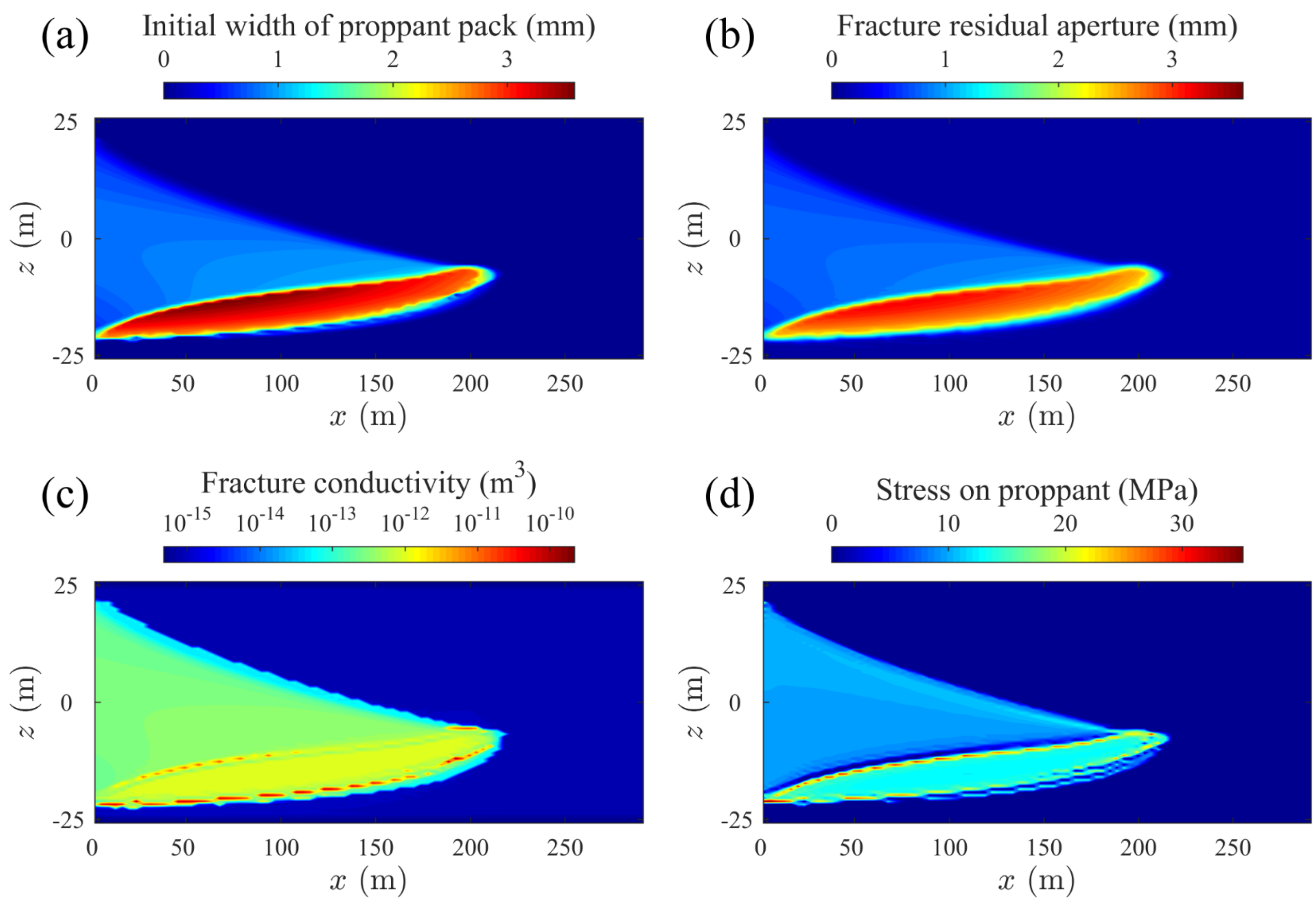

p_f = 10 MPa

(a) Initial width of proppant pack, (b) fracture residual aperture, (c) resultant fracture conductivity, and (d) stress applied on proppant packs.

Numerical Results: 2D cases

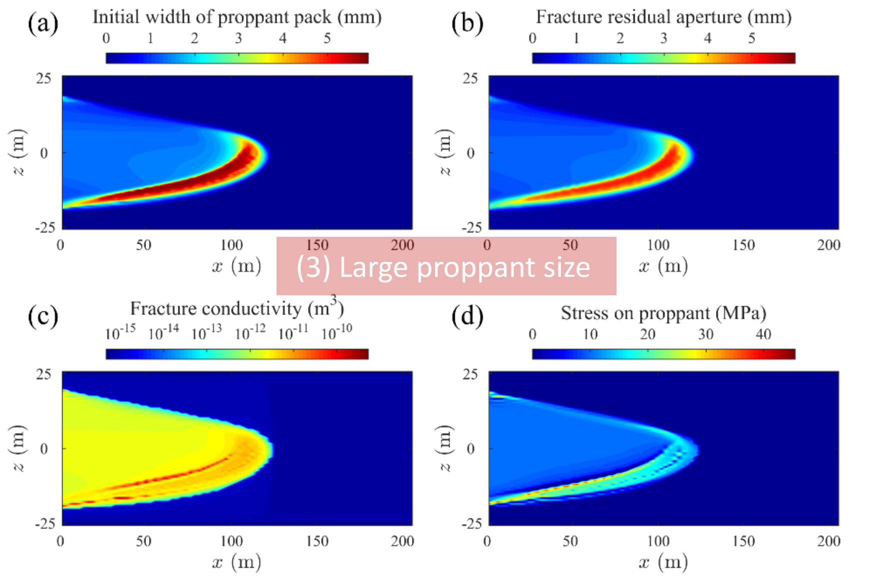

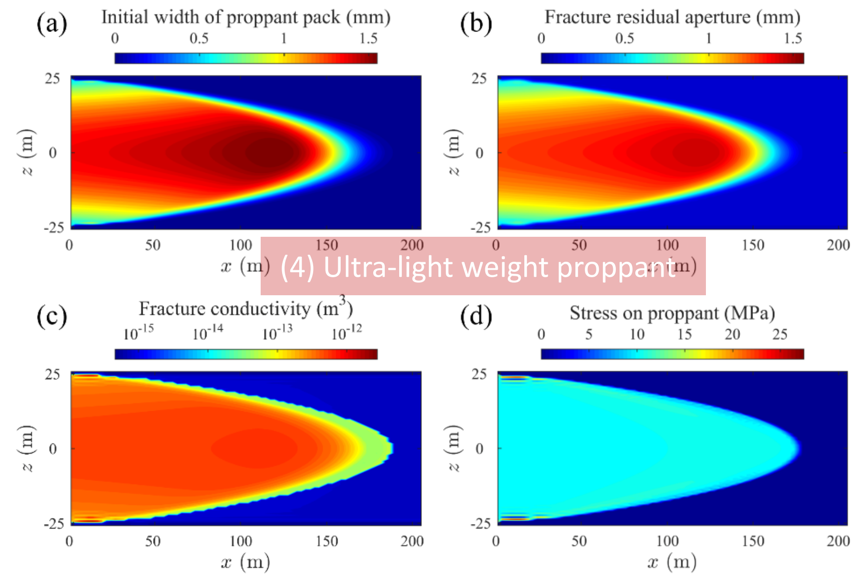

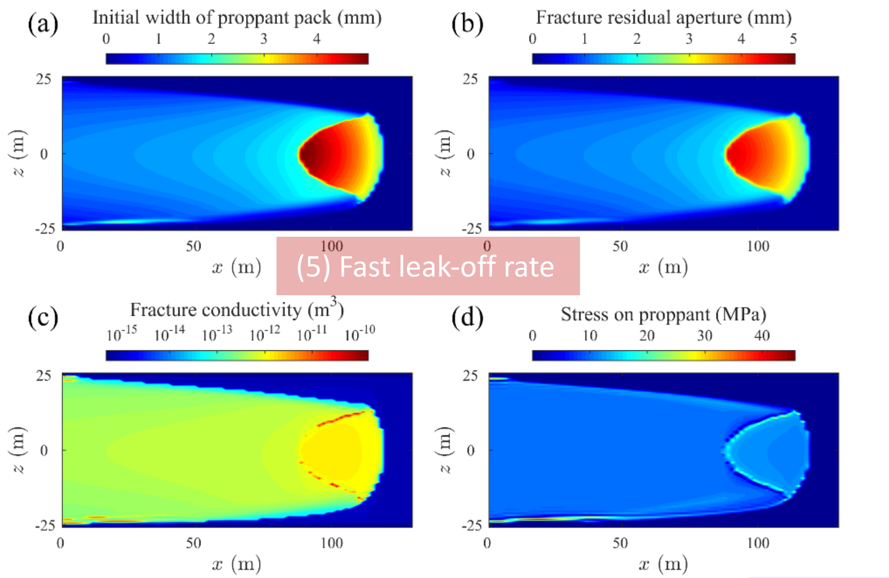

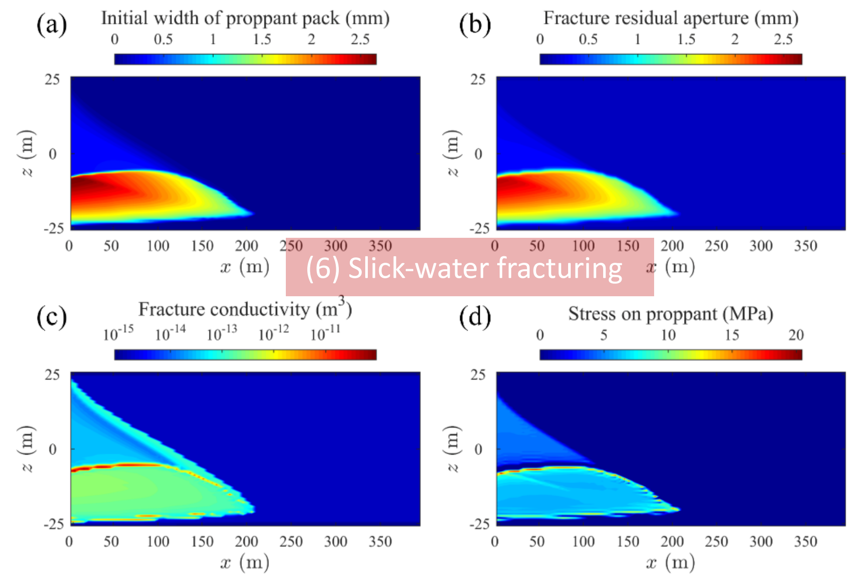

p_f = 10 MPa

Numerical Results: Reservoir Simulation

Reservoir Simulation

- Gas flow in the reservoir

$$\phi_{rsv}\rho_g c_g \frac{\partial p_{rsv}}{\partial t} + \nabla \cdot \left(-\frac{k_{rsv}}{\mu_g} \rho_g \nabla p_{rsv} \right) = 0$$

All boundaries are set as no flow, except for $p_{rsv}(x,z)\big|_{y=0} = p_f(x,z)$

- Gas flow in the hydraulic fracture

$$w_r \varphi_r \rho_g c_g \frac{\partial p_f}{\partial t} + \nabla \cdot \left(-\frac{C_f}{\mu_g} \rho_g \nabla p_f \right) = \boxed{2\frac{k_{rsv}}{\mu_g} \frac{\partial p_{rsv}}{\partial y}\bigg|_{y=0}}$$

All boundaries are set as no flow, except that a production well (constant BHP) locates at (0,0,0)

Initial condition: Constant pressure

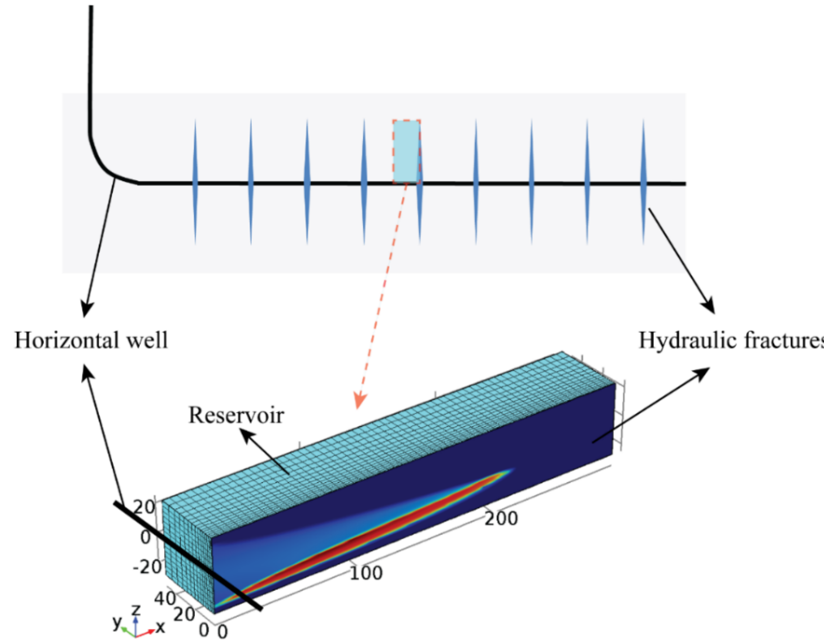

Table 3. Input parameters for the reservoir simulation.

Parameters	Values
Fracture spacing, s_f	100 m
Diameter of the wellbore, d_w	0.25 m
Porosity of the reservoir, φ_{rsv}	0.1
Permeability of the reservoir, k_{rsv}	1×10^{-17} m^2
Initial pore pressure, p_{rsv0}	20 MPa
Dynamic viscosity of methane, μ_g	1.19×10^{-5} Pa·s
Bottomhole pressure (BHP), p_{BHP}	3 MPa

Numerical Results: Reservoir Simulation

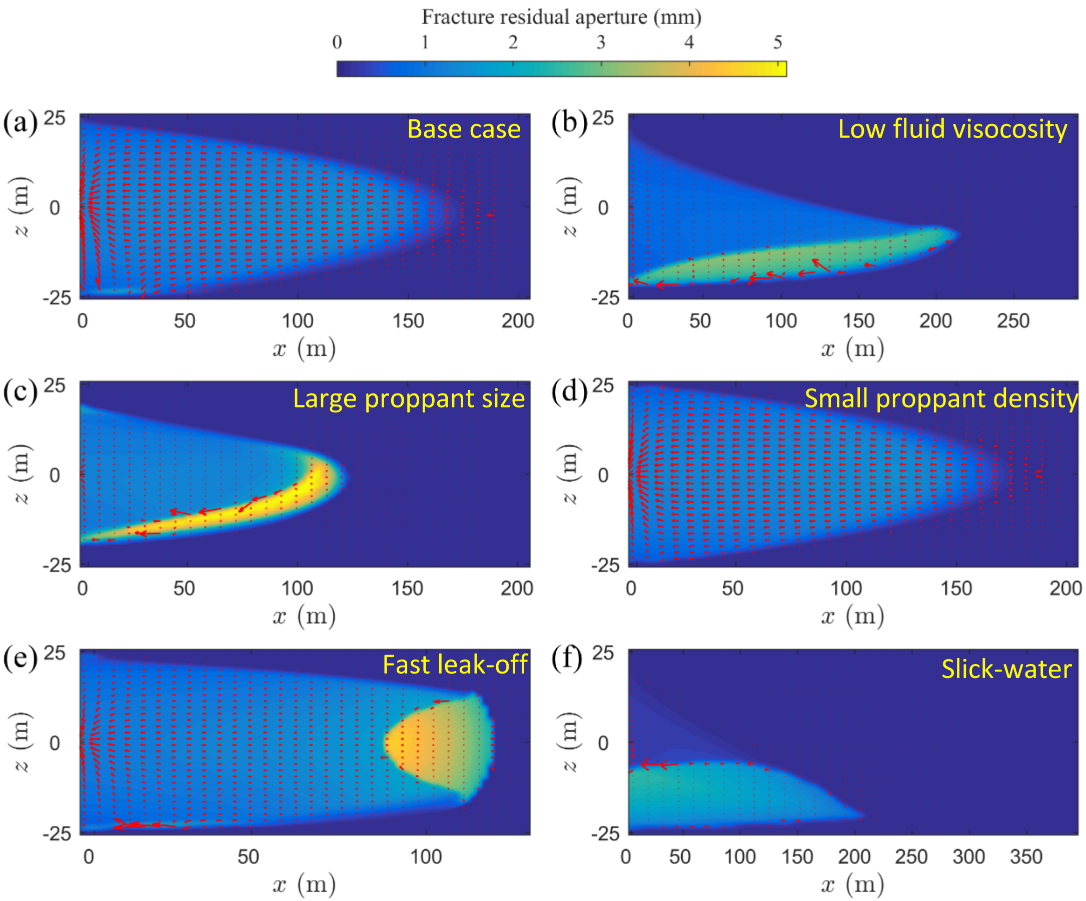

Fluid flow paths in the hydraulic fractures for different cases when productions last 1 year.

Best performance:

4 – Lightweight proppant

1 – Water (non-slickwater)

.....

6 - Slickwater

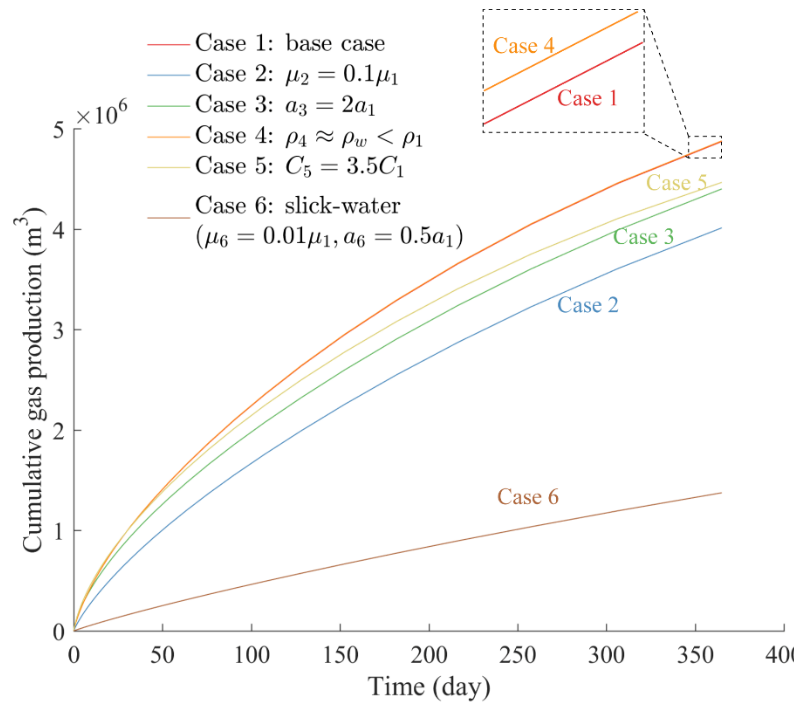

Cumulative gas production versus time

Propagation, Proppant Transport and the Evolution of Transport Properties of HFs

- Static Gas Fracturing
  - Rationale for Its Use
  - Physical Characteristics and Key Observations
  - Methods of Analysis
  - Unresolved Issues
- Key Connections to Dynamic Gas Fracturing
  - Key observations
  - Essence of Dynamic Response
  - Zeroth- and First-Order Models
- Proppant Transport in Gas Fractured HFs (Jiehao Wang)
  - Deformation-Transport-Closure Models
  - Observations
- Evolution of Permeability in HFs (Jiehao Wang)
  - Closure-Compaction and Arching
  - Productivity Controls
- **Microbially Enhanced CBM (Sheng Zhi)**
- Summary

Optimizing Nutrient Delivery in Microbially Enhanced Coalbed Methane (MECBM) Reservoirs

Sheng Zhi, Derek Elsworth

52nd US Rock Mechanics/Geomechanics Symposium

Date: 06/20/2018

Overview

- Background
- Methodology
- Reservoir Modelling and Results
- Conclusions
- Reference

Background

- **Definition of CBM**

  Natural gas produced from coal seams

- **Producing areas**

  The San Juan Basin, Powder River Basin, Black Warrior Basin and Central Appalachian Basin

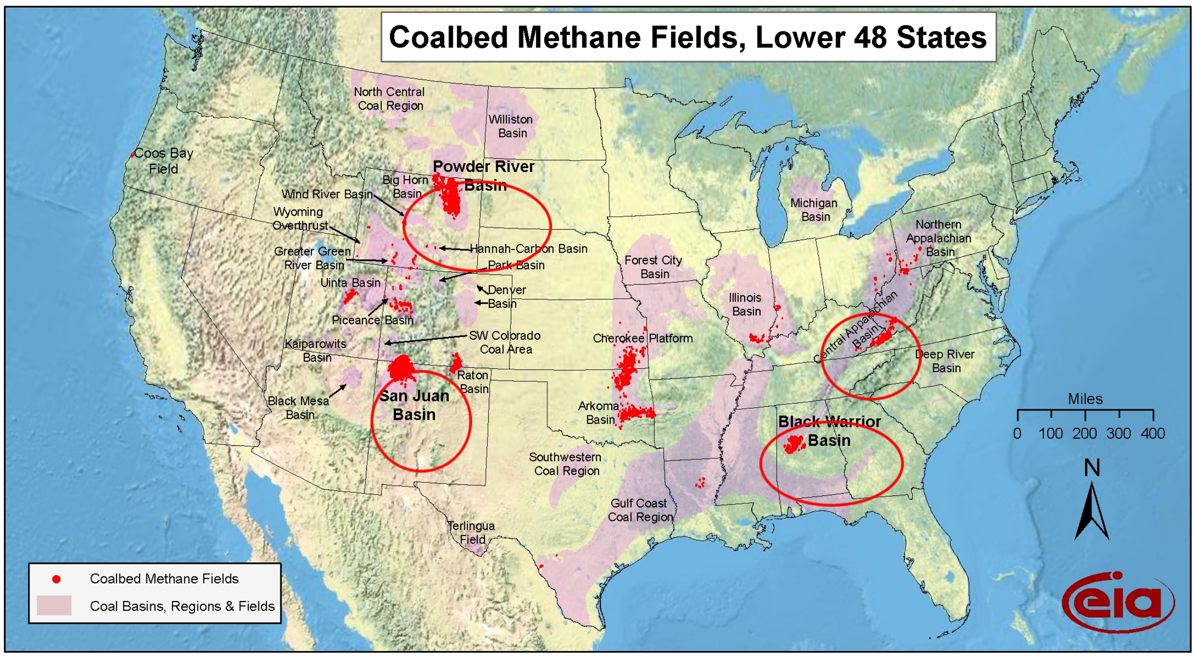

Source: Energy Information Administration based on data from USGS and various published studies
Updated: April 8, 2009

1269 BCF in 2015

~5% to ~9% of annual natural gas production since 2001

PennState

Background

- **Microbially enhanced coalbed methane (MECBM)**

  Active microbial methanogenesis in coal seams

- **Benefits**

  To yield more methane

  To increase lifespan of existing CBM wells

  To generate gas in non-producing CBM wells

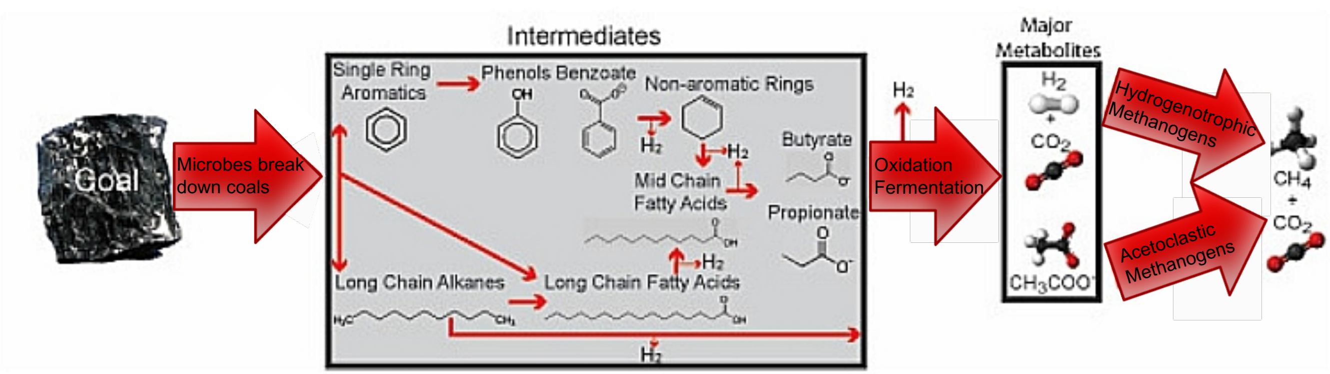

Steps for biodegradation of coal to methane (*Ritter et al., 2015*).

Background

Laboratory-scale experiments

Biogenetic methane production after different periods (*Zhang et al., 2016*).

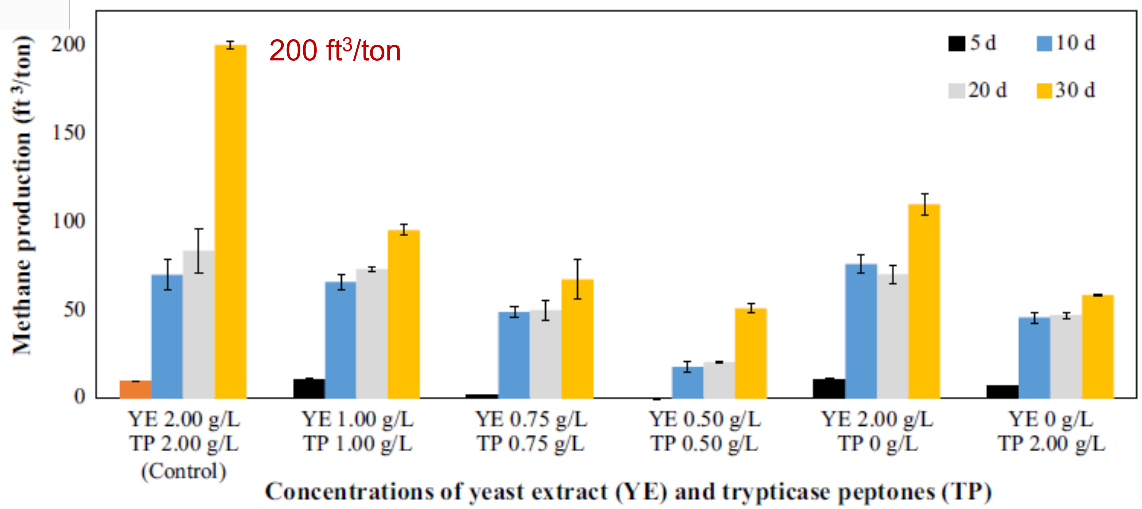

Powdered coal sample

+Methanogentic Archaea

+Nutrient

Components of nutrient:

- ✓ Mineral ions: Mg^{2+}, Ca^{2+}, K^{+}, Na^{+}
- ✓ Organic matters: Yeast and peptone
- ✓ Vitamin solutions: B12, B3, thioctic acid

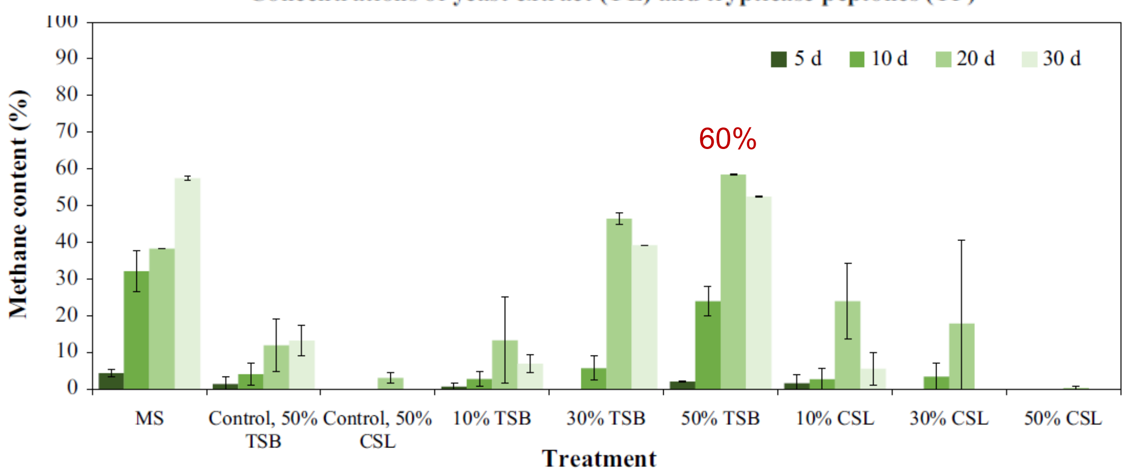

Volumetric methane contents in reactor after different periods (*Zhang et al., 2016*).

Background

Field-scale practice

Corporation: Luca Technologies, Inc., Next Fuel, Inc., Ciris energy, Synthetic Genomics, Inc., ExxonMobil, Arctech

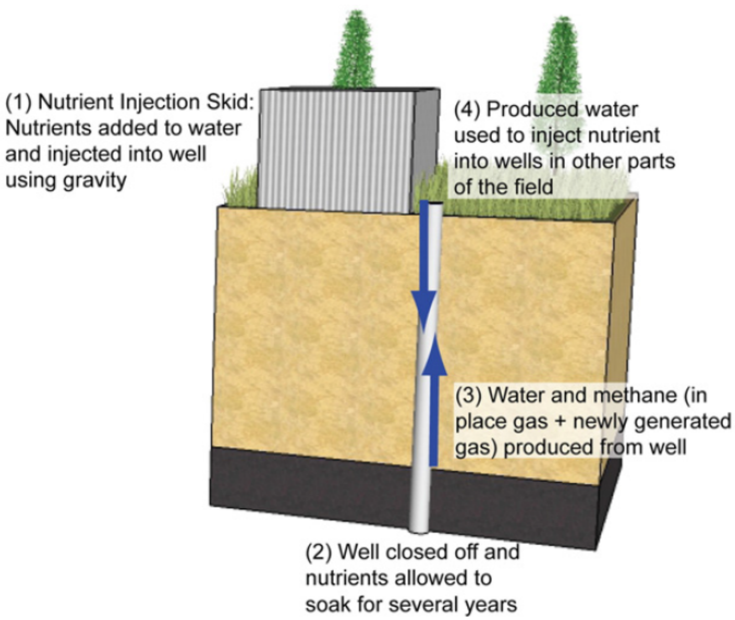

Stimulation methods for biogenetic methane production (*Ritter et al., 2015*).

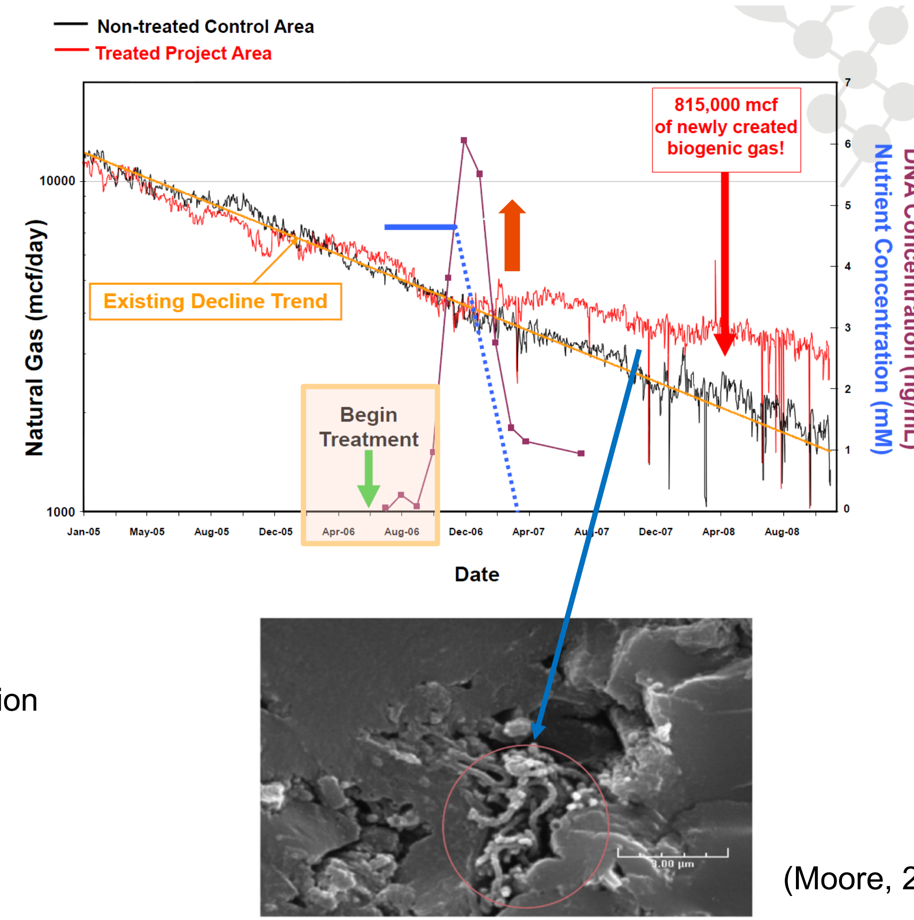

(Moore, 2012)

Overview

- Background
- Methodology
- Reservoir Modelling and Results
- Conclusions
- Reference

Methodology

Reservoir modeling

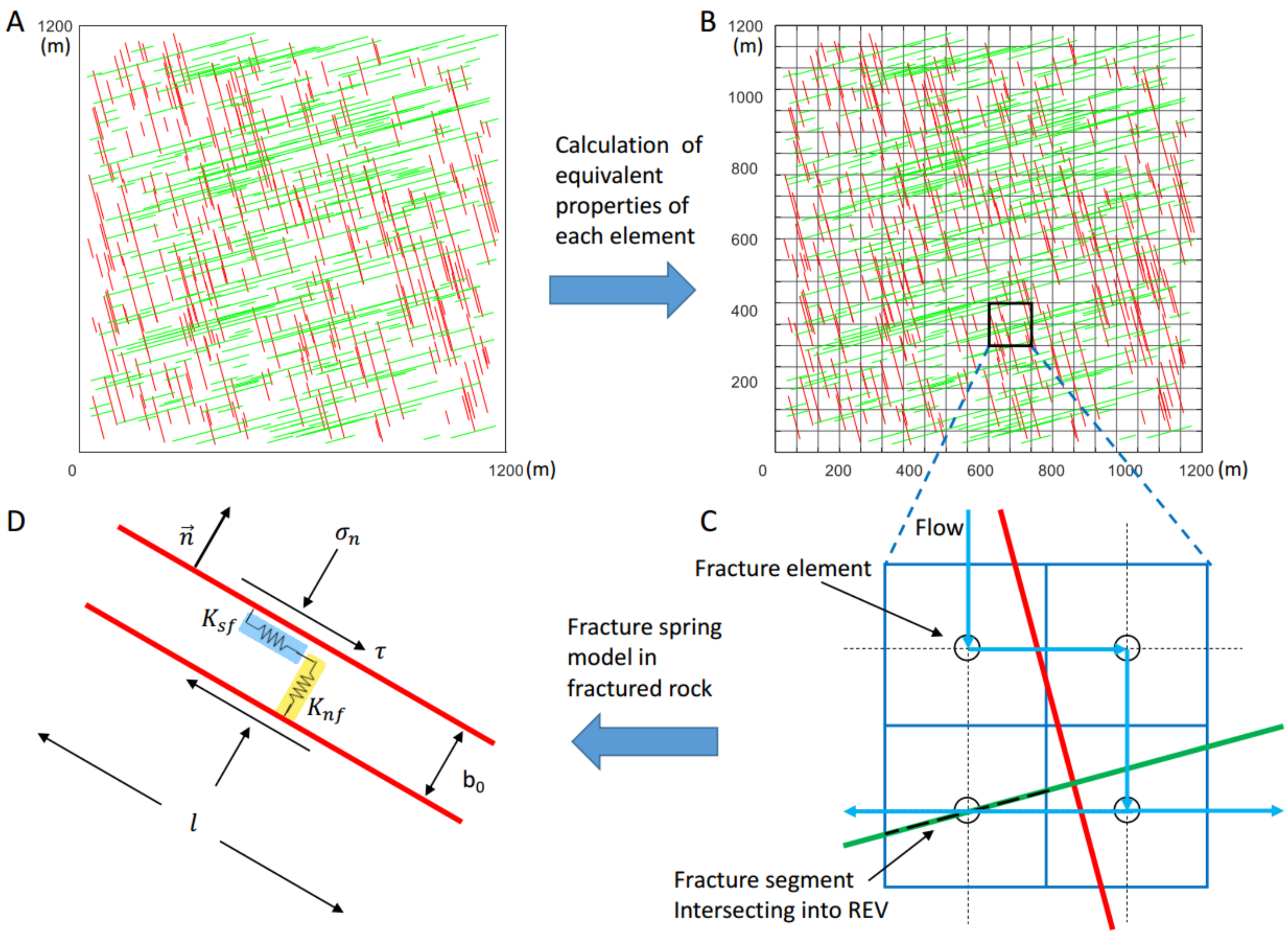

Scheme of equivalent continuum method used in this study.

Methodology

DFN generation and important parameters in this studyin

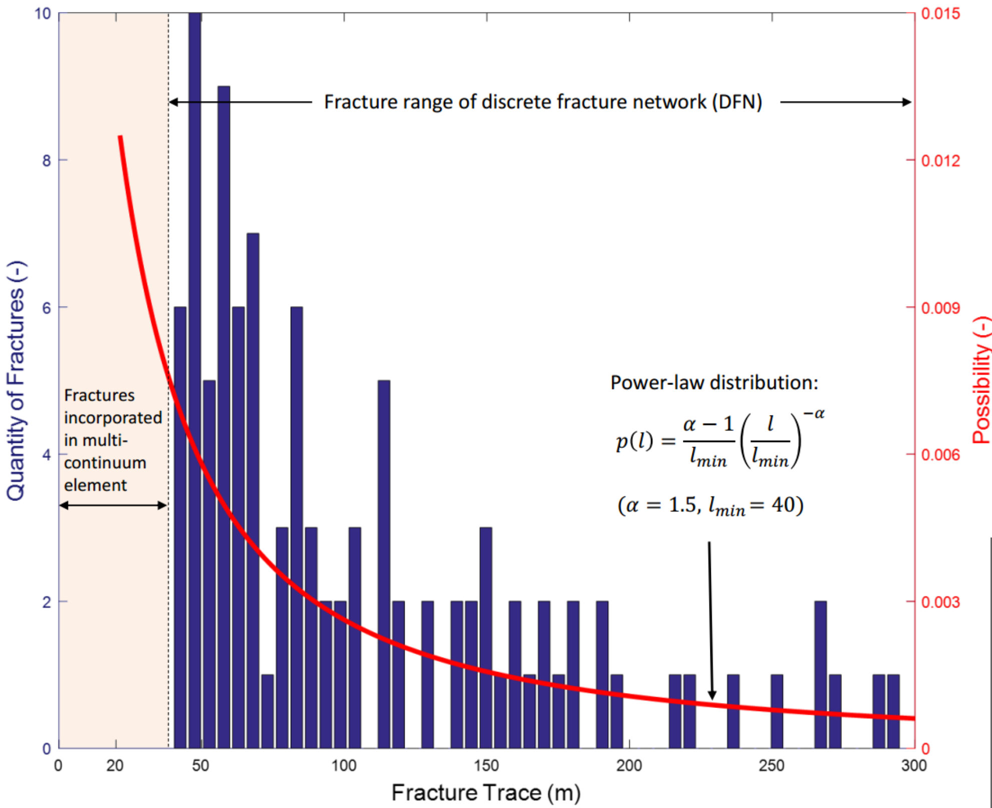

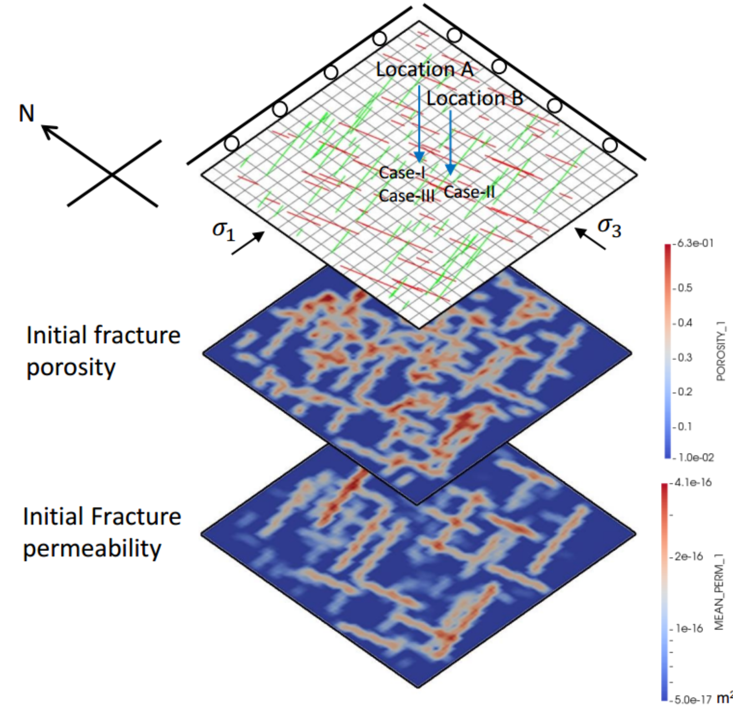

Two sets of orthogonal fracture at azimuths of 075° and 165° (from the North)

Table 2. Modeling parameters for hydraulic fracturing	
Parameter	Value
Young's modulus of coal (, GPa)	2.45
Poisson's ratio of coal (, -)	0.34
Fluid dynamic viscosity (,)	0.2
Injection flow rate (,)	0.05
Coal seam thickness (, m)	10
Fracture height (, m)	10
Biot's coefficient (, -)	
Maximum confining stress (, MPa)	20 (E-W)
Minimum confining stress (, MPa)	16 (N-S)
Initial reservoir pressure(, MPa)	1.0
Pre-existing fracture angle ()	75/-15

Methodology

How will fracture change during EMCBM production?

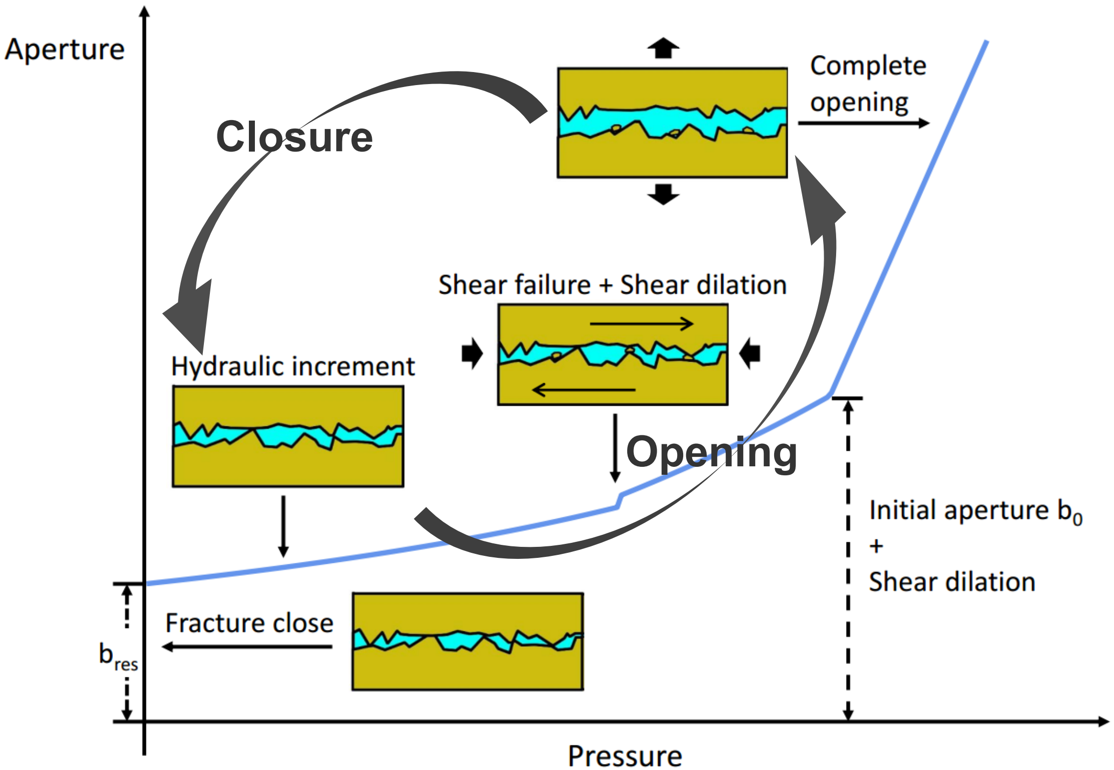

Schematic of fracture aperture evolution.

Hydraulic increment:

where , b_0 is the initial aperture, is the effective stress.

Shear dilation:

where is the shear stiffness, is the dilation angle

Mechanical opening (complete open):

where is shear modulus, is normal stress on fracture surface

Methodology

The proposed PKN model

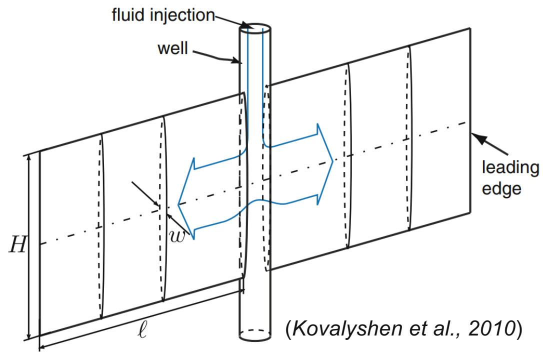

(*Kovalyshen et al., 2010*)

The lubrication equation

The average local flux

The leak-off in Carter's model

The global equation

Parameter	Value
Young's modulus of coal (E)	2.45 GPa
Fluid dynamic viscosity (μ)	0.1 $\mathrm{Pa \cdot s}$
Injection rate (Q_o)	0.05 $\mathrm{m^3/s}$
Poisson's ratio of coal (ν)	0.25
Height of coal seam (H)	10 m
Leak-off coefficient (C_l)	$5e-5\ \mathrm{m \cdot s^{1/2}}$

Table 3. Modeling parameters for the validation of proposed PKN

The global equation (with pre-existing fracture at inlet)

the small time asymptotic solution

where the corordinate ,

the large time asymptotic solution

(*Nordgren, 1972*)

where

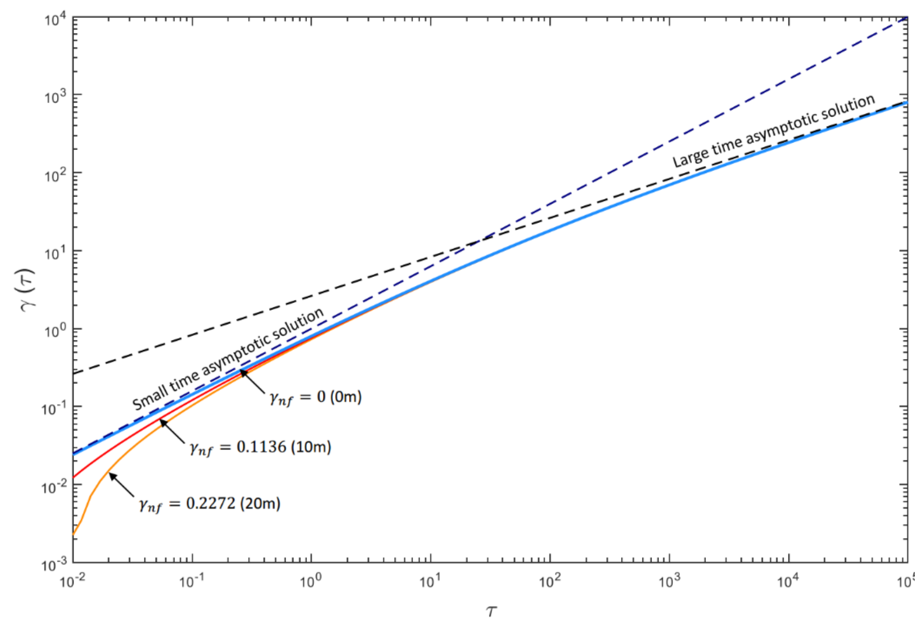

Methodology

Hydraulic fracture propagation in CBM reservoir

Three assumptions in the model are made (X. Zhang & Jeffrey, 2014):

- The hydraulic fracture may re-initiate from the branched tip of a natural fracture when it meets the propagation criterion.
- The deflection angle is negligible because the growing fractures tend to quickly align themselves to be parallel to the maximum principal stress.
- Two new proximal fractures (separation smaller than element size) will merge to form a larger fracture.

LEFM propagation criterion:

A mixed stress intensity factor > the toughness at the onset of quasi-static crack growth.

$$K_{IC} \geq K_I + K_{II}$$

where

$$K_I = \frac{2}{\sqrt{3}}\sigma_n^{'}\sqrt{\pi a} = \frac{2}{\sqrt{3}}(\sigma_n - p_f)\sqrt{\pi a}$$

$$K_{II} = \frac{2}{\sqrt{3}}(\tau - \mu\sigma_n^{'})\sqrt{\pi a}$$

The critical fluid pressure when tension-shear wing fractures initiate:

$$p_{fc} = \sigma_n - \left(\sqrt{\frac{3}{4\pi a}}K_{IC} - \tau\right) / (1 - \mu_f)$$

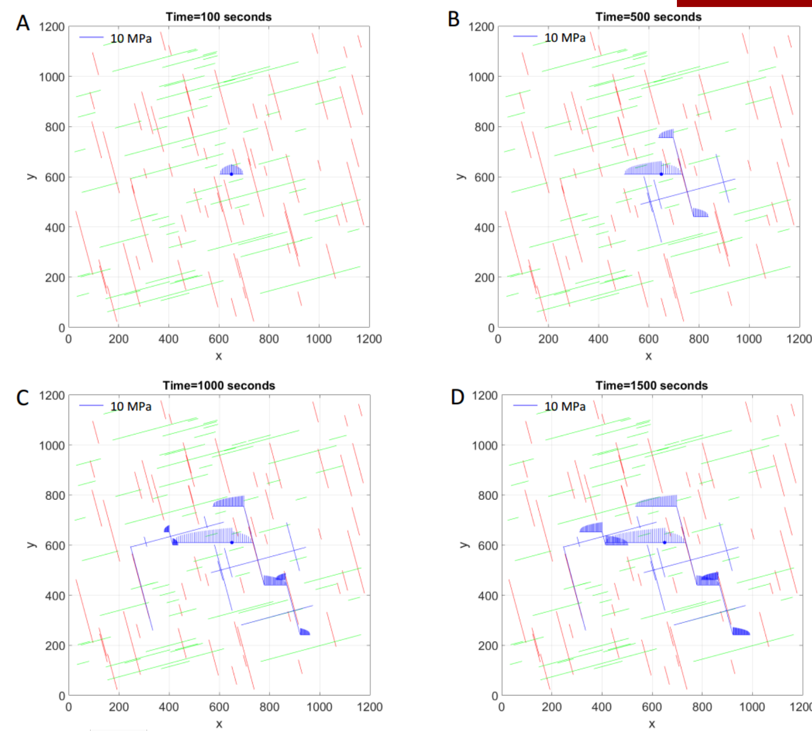

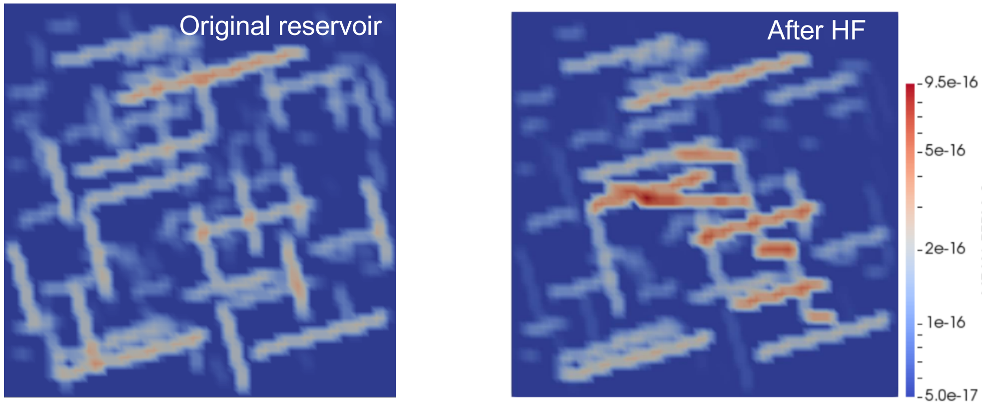

Methodology

CBM reservoir after HF stimulation

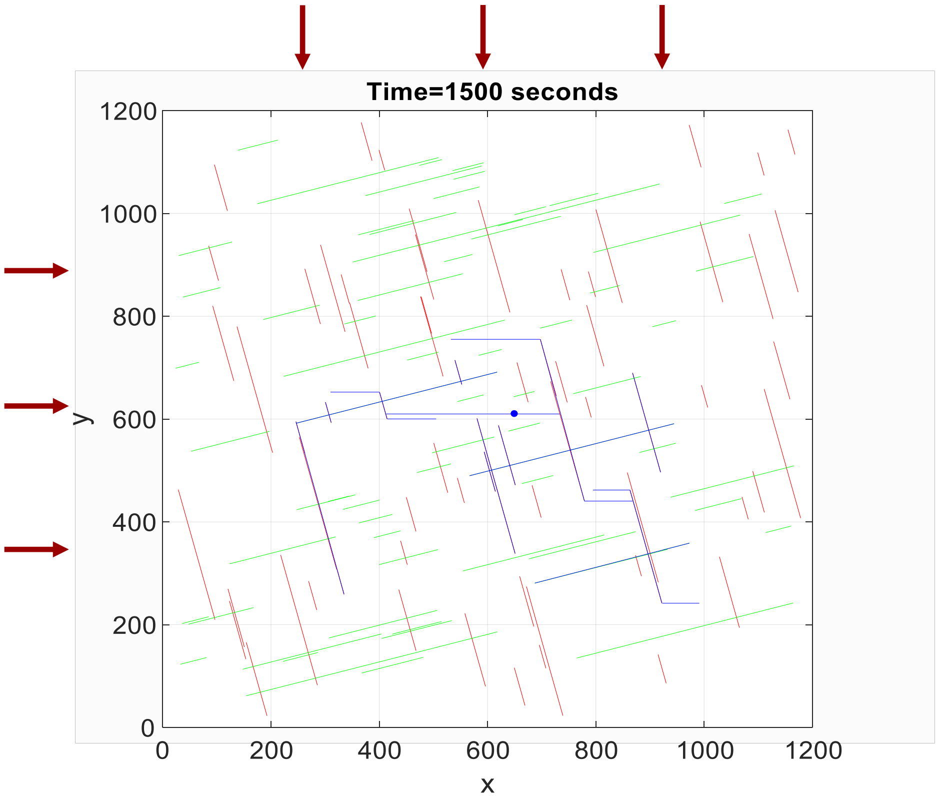

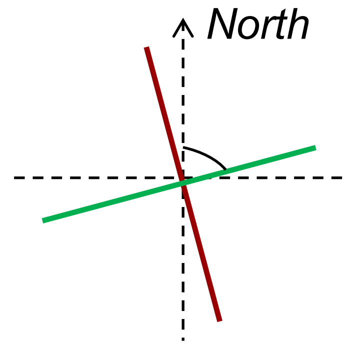

Fracture permeability distribution (before injection)

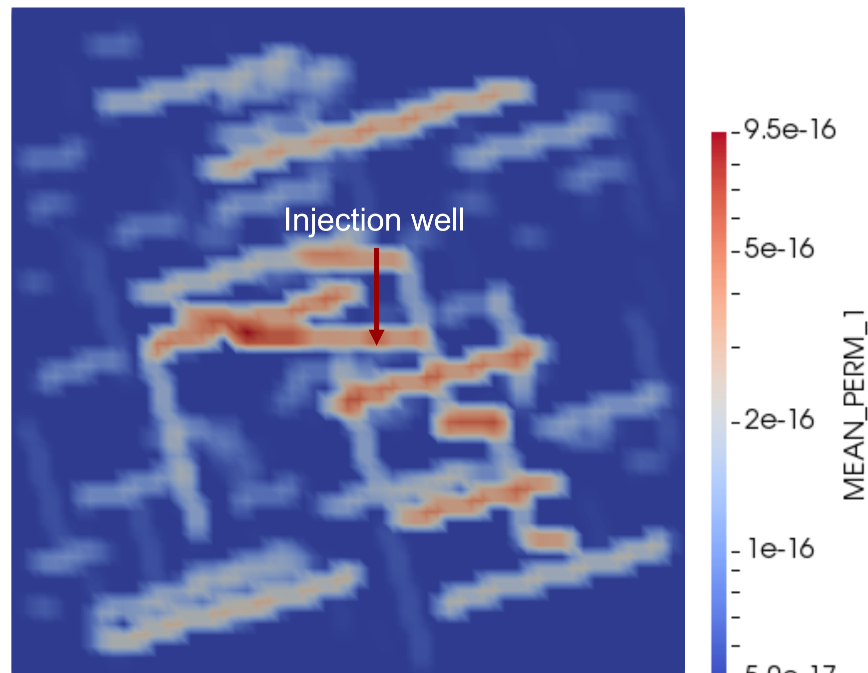

- Two sets of orthogonal fracture at azimuths of 075° and 165° (from the North)
- ,

Methodology

Solution transport:

General Advection-Diffusion Equation for the porous medium:

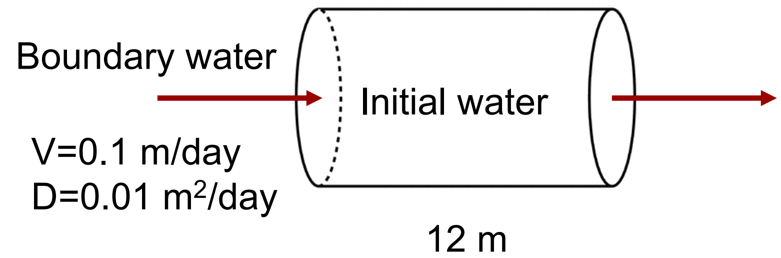

where C_{jk} is the tracer concentration for j-th component, D_h is the combined dispersion–diffusion tensor.

Model in TFReact simulator

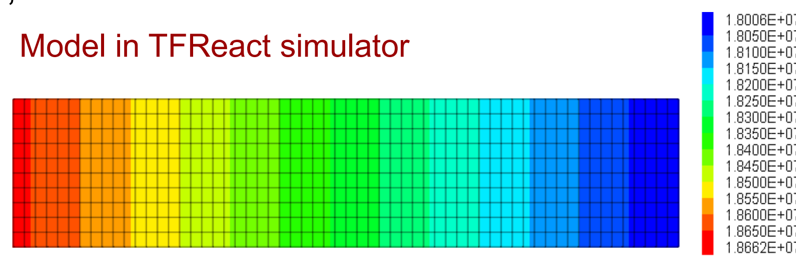

where D_e is the effective diffusion coefficient, D_m is mechanical dispersion coefficient.

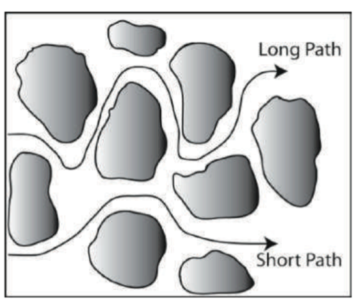

(*Steefel and Maher, 2009*)

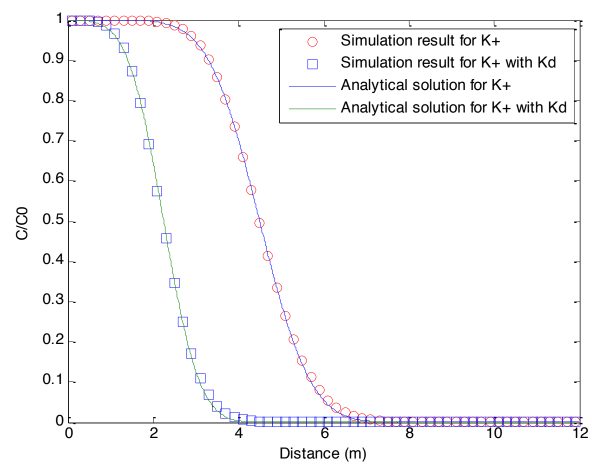

Simulation results vs. analytical results for K^+ with and without retardation factor R =2.0 after 40 days

Overview

- Background
- Methodology
- Reservoir Modelling and Results
- Conclusions
- Reference

PennState

Reservoir modeling and Results

Nutrient distribution

Case-I: Injection through matrix

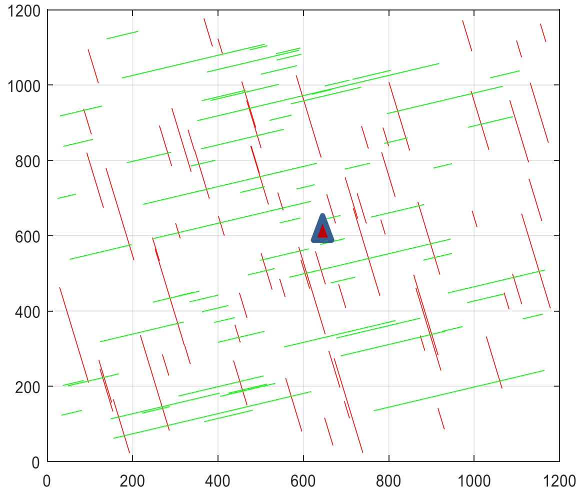

Case-II: Injection through NFN

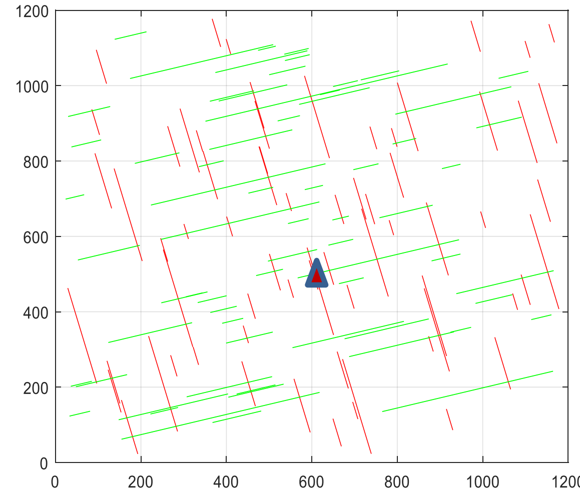

Case-III: Injection through HF+NFN

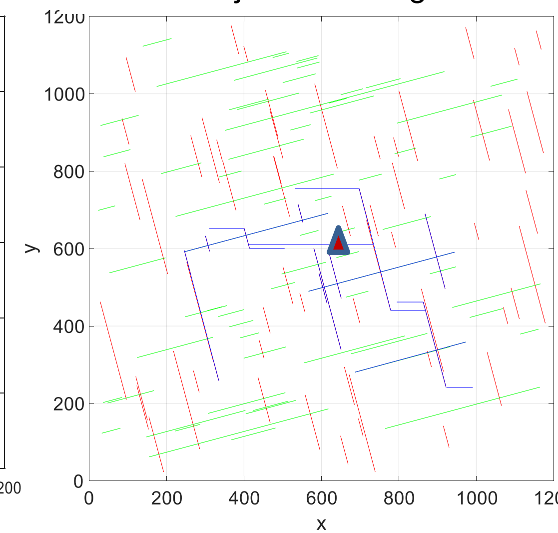

After 30-day injection

Case-I

Time=30 days

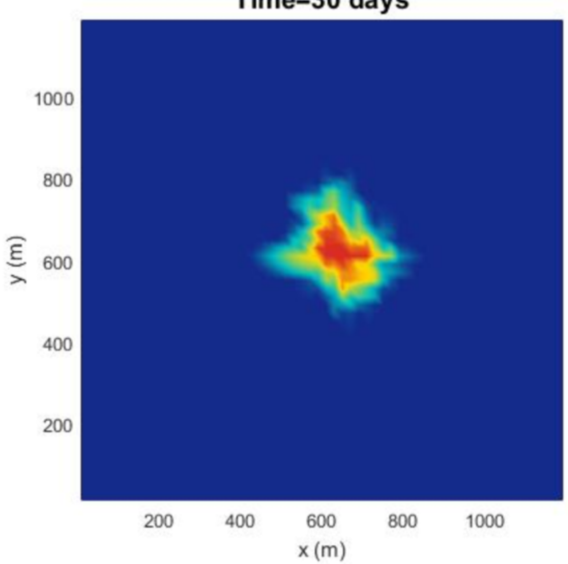

Case-II

Time=30 days

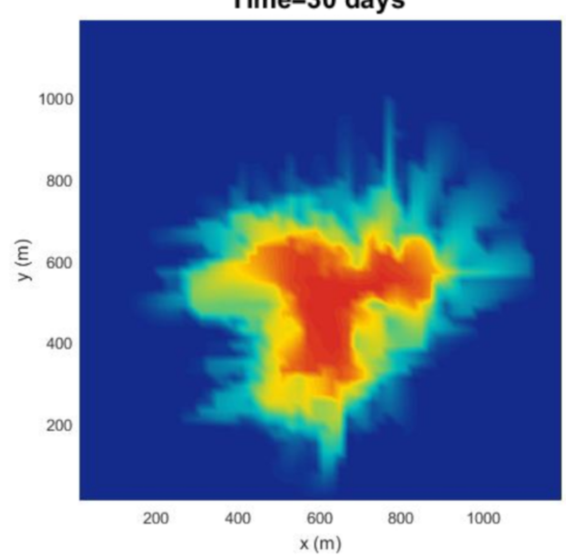

Case-III

Time=30 days

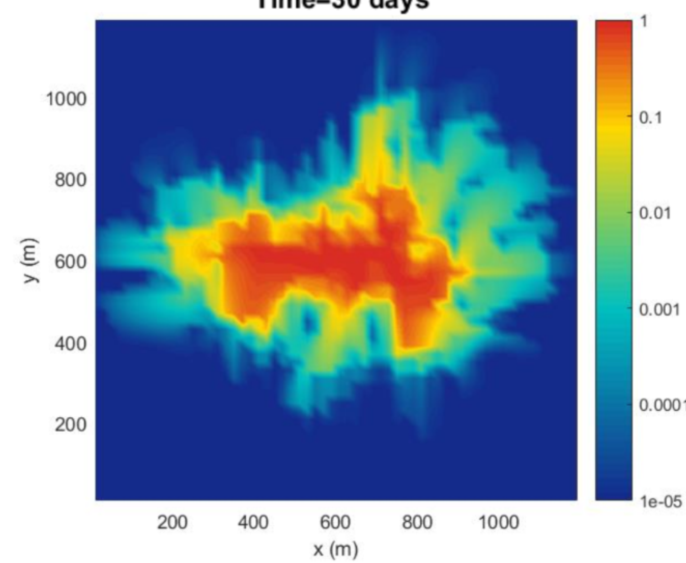

Reservoir modeling and Results

Nutrient distribution

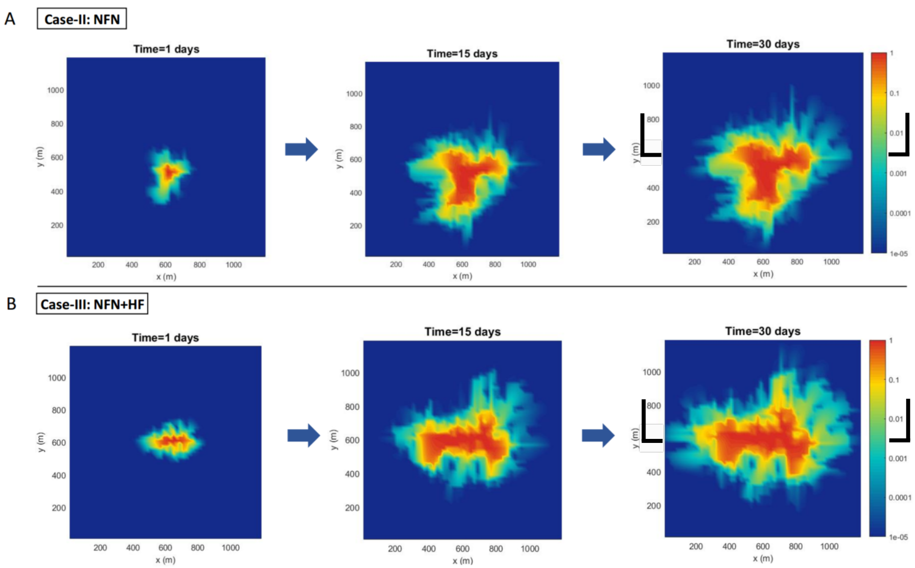

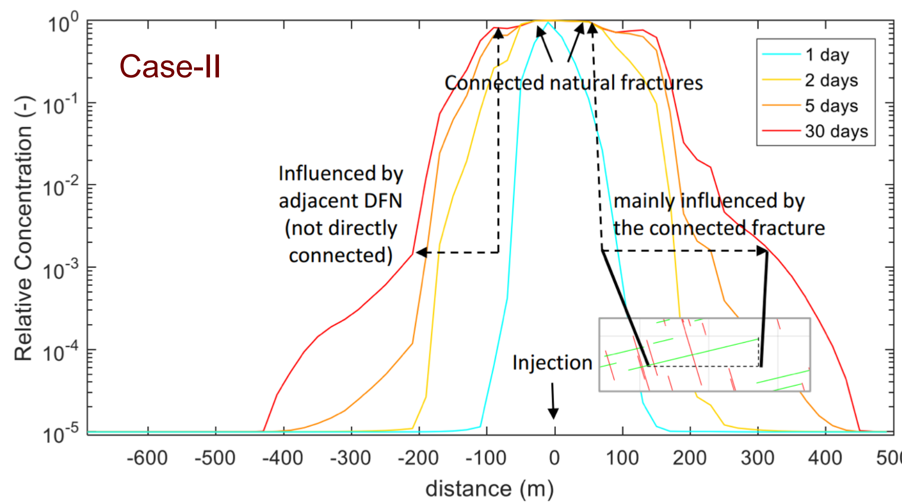

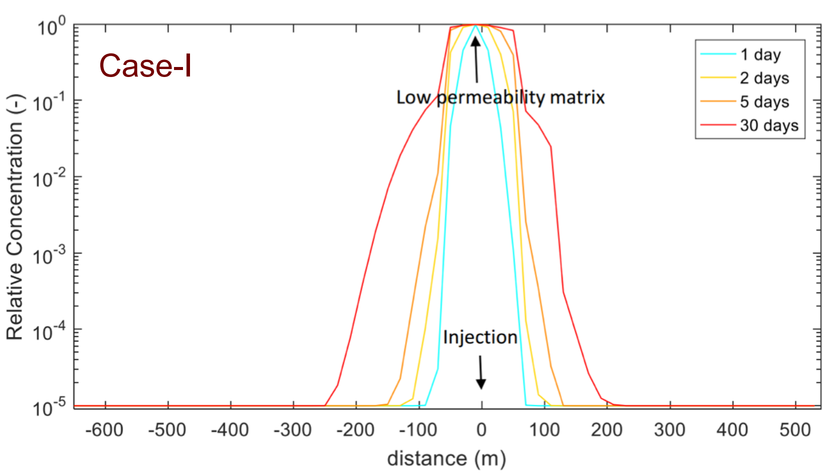

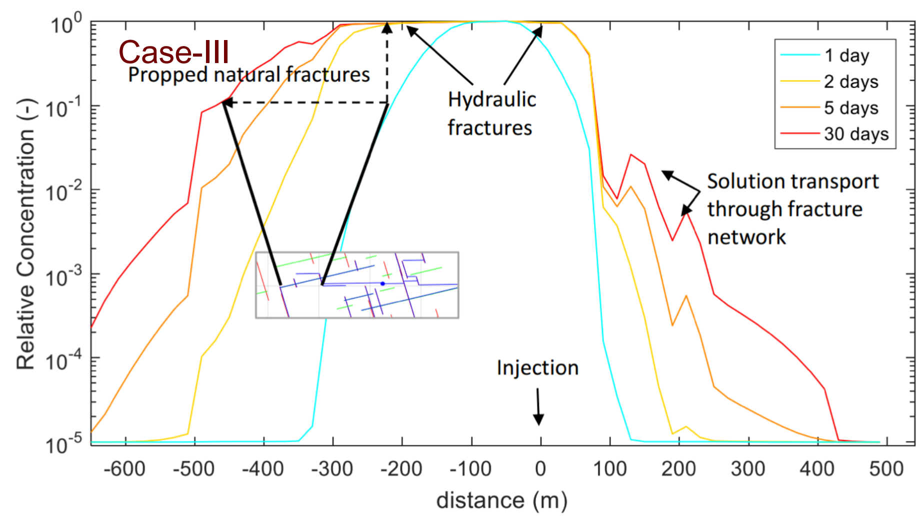

Fracture modeling and Results

Solute transport in different fracture types

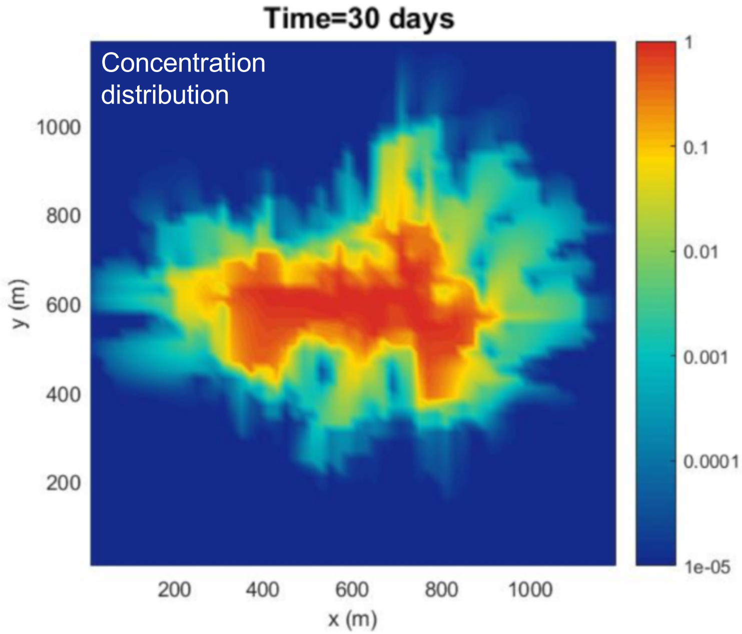

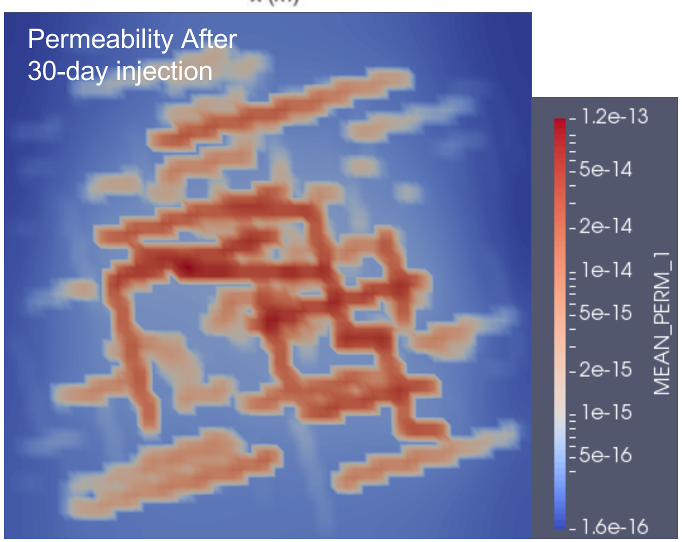

4 locations selected in three cases to represent different fracture types and matrix (Distance to inlet = 80 m)

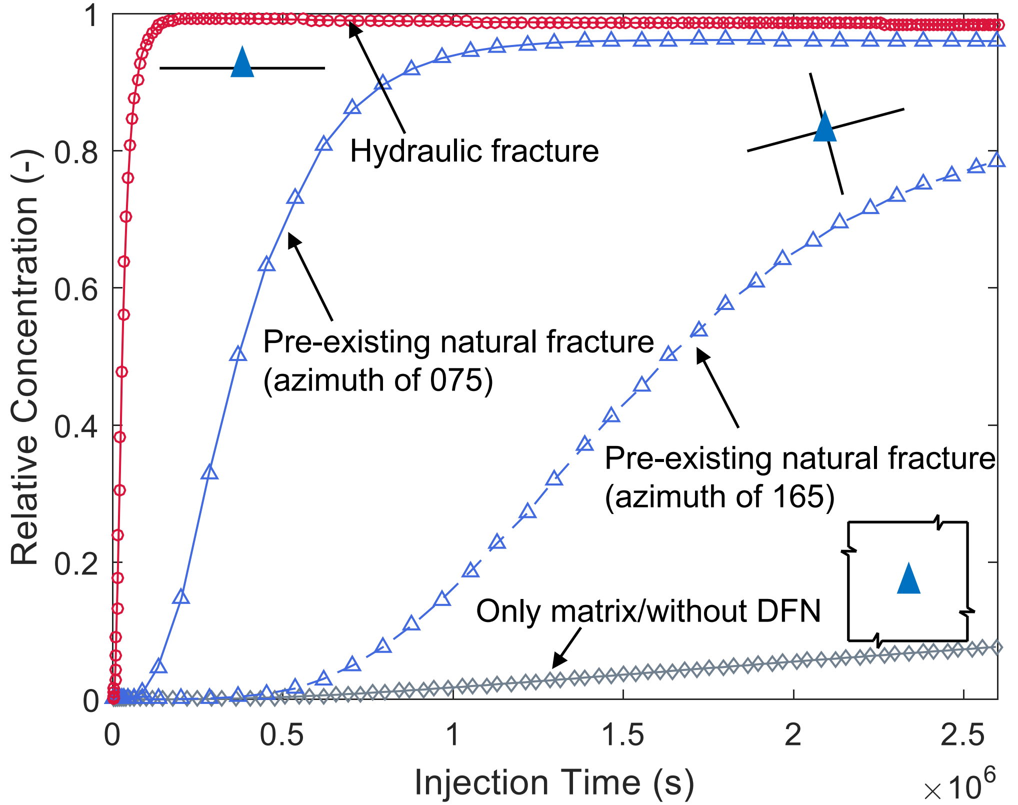

hydraulic fractures will provide the most effective pathways for aqueous mineral transport

Fracture modeling and Results

Mineral concentration changes in hydraulic fracture

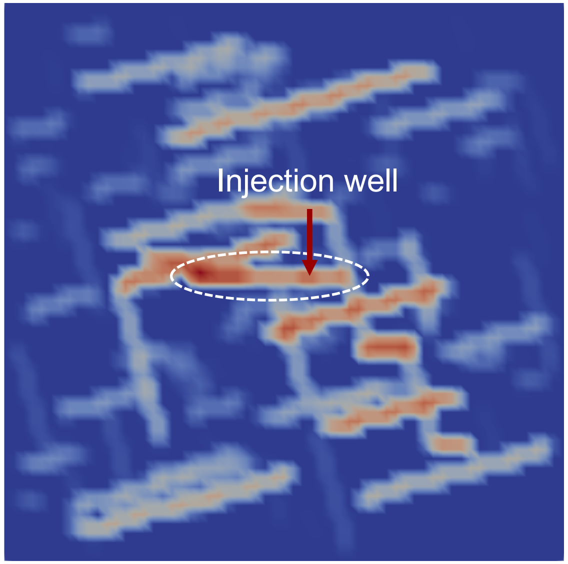

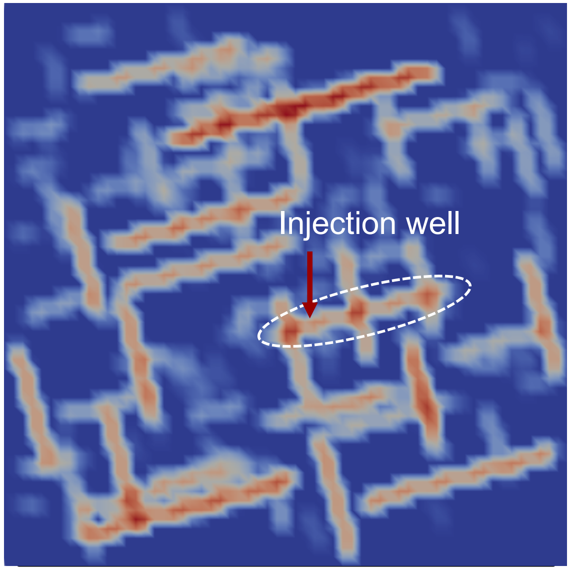

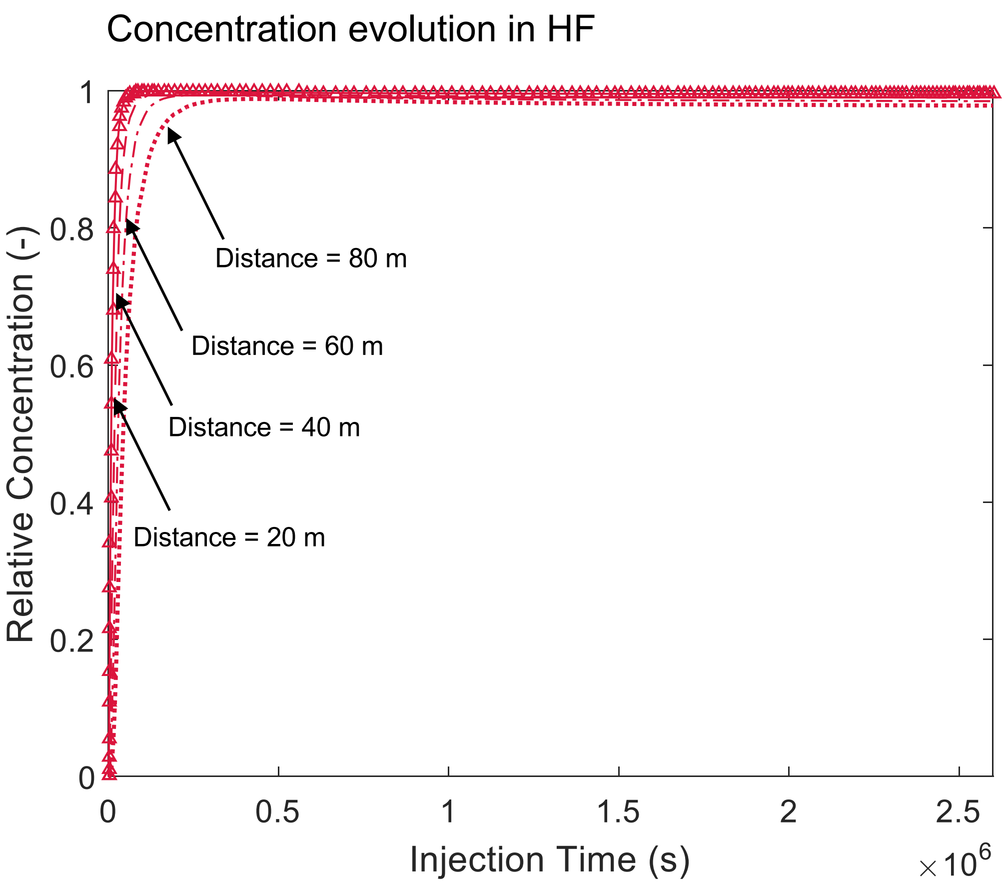

Delivery capability of hydraulic fracture slightly decreases with distance.

Fracture modeling and Results

Mineral concentration changes in natural fracture

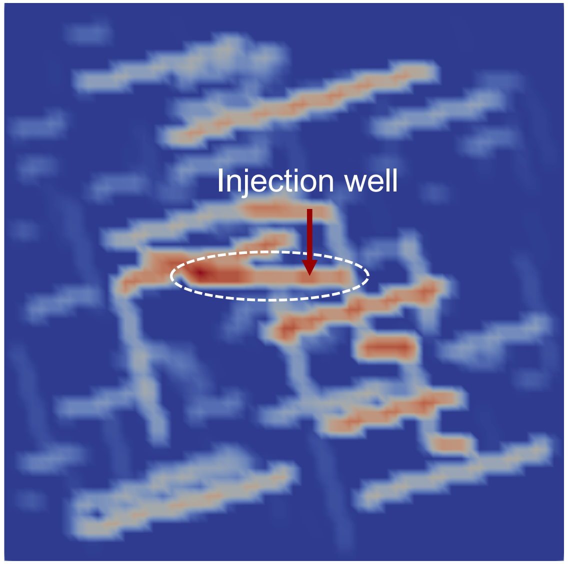

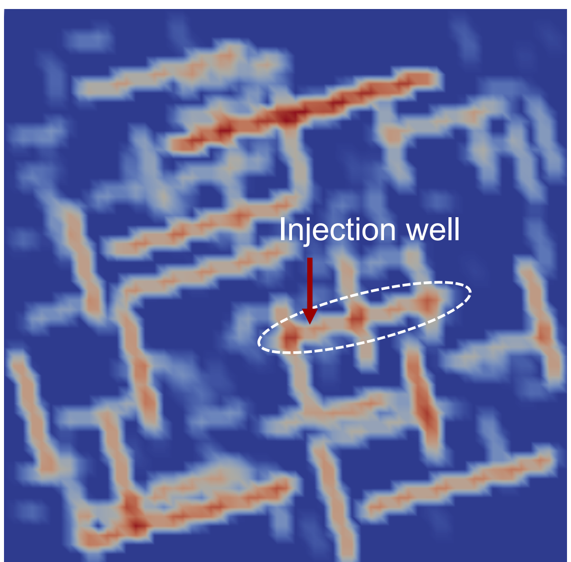

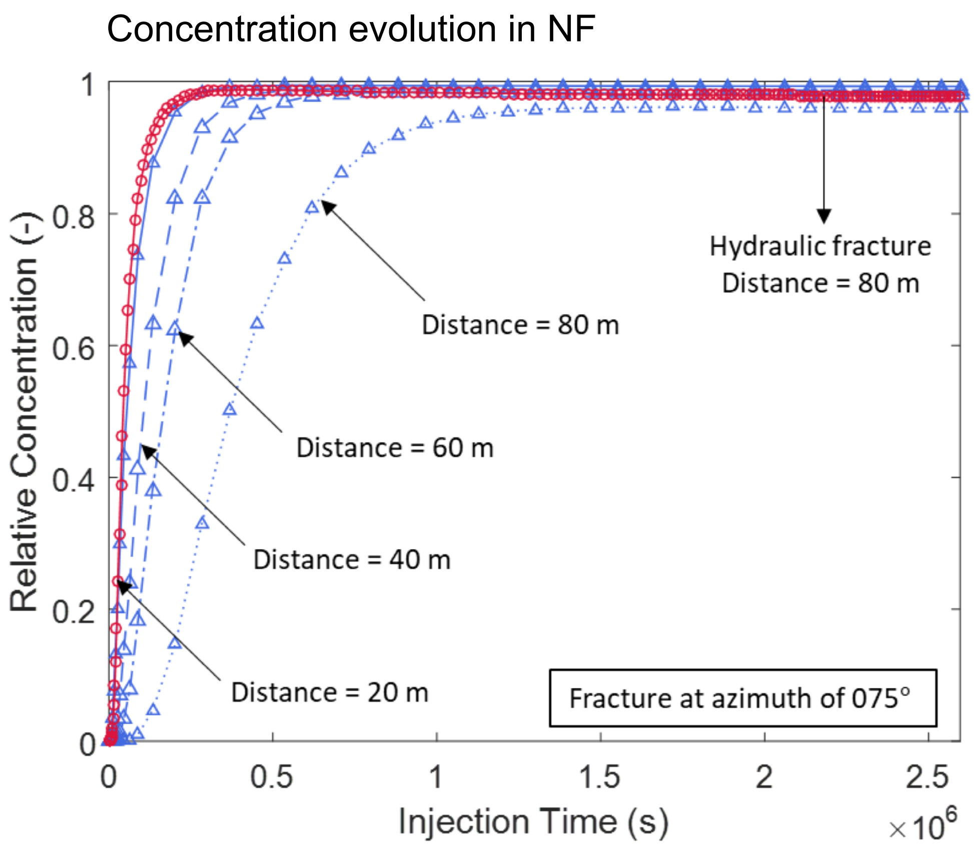

Delivery capability of pre-existing fracture largely decreases with distance.

Reservoir modeling and Results

Mineral abundance

Totally four concentration levels in the range from 0.0001 to 1 at interval of 10 folds.

RC>0.1 RC>0.01 RC>0.001 RC>0.0001

For each multi-continuum element, Saturated cleat area (SCA) can be calculated by

where is the quantity of discrete fractures within n-th element. is the element volume. and are the intercepted fracture length and aperture of n-th fracture, respectively. A_0 is the cleat area per ton of coal.

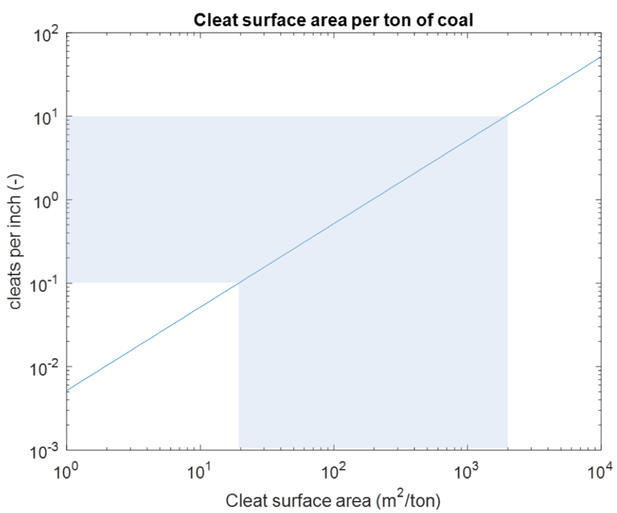

Saturated cleat area at different concentration levels for the three cases

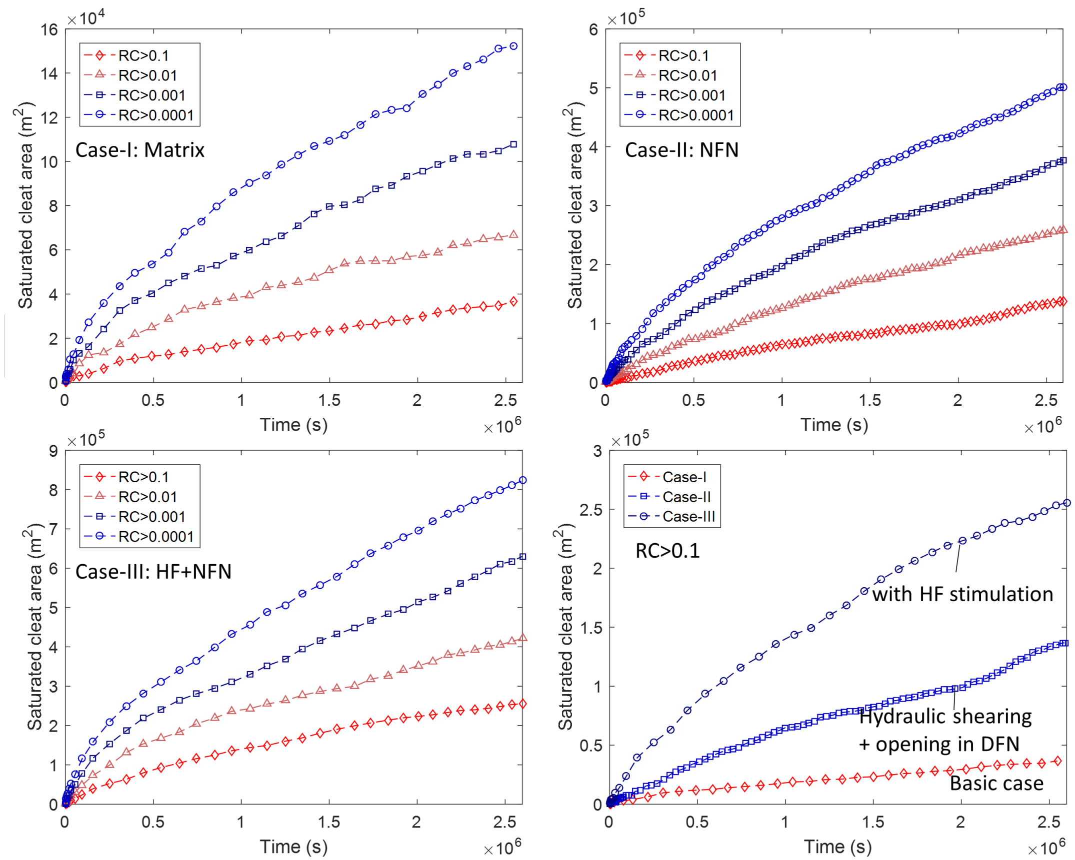

A_0 is considered as 600 m^2/ton in this study

Reservoir modeling and Results

Mineral abundance

Cumulative nutrient volume injected in 30 days

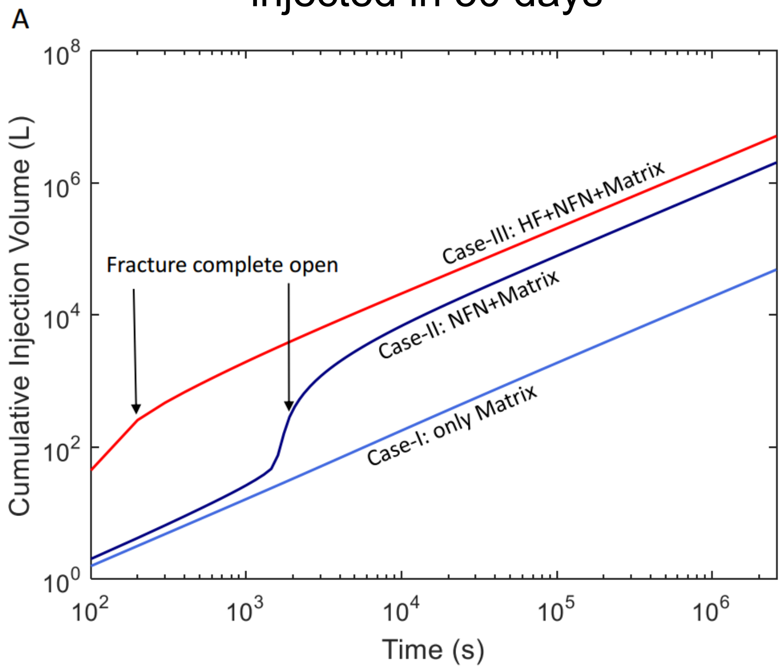

(A) Cumulative injected volume of nutrient versus injection time.

Injection rate change during 30-day injection (=22MPa)

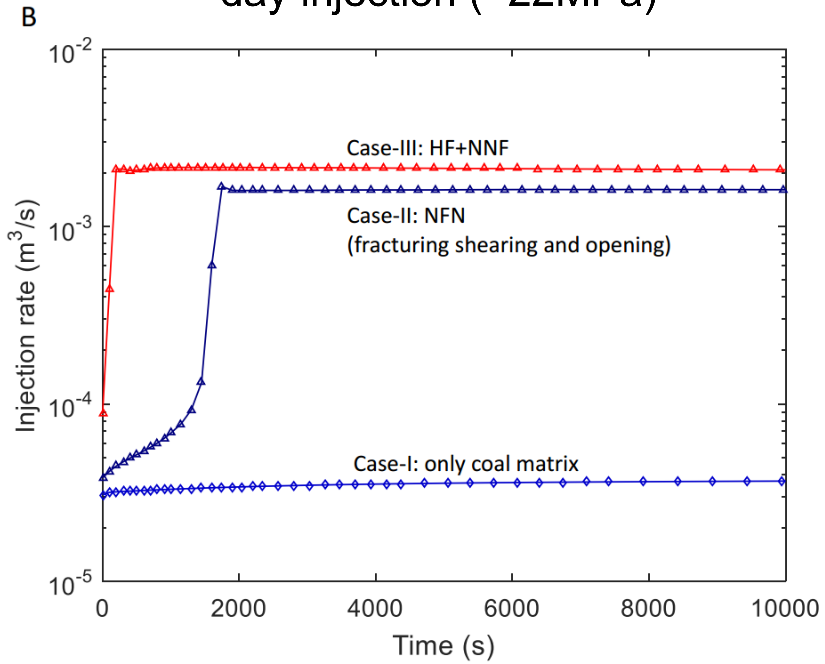

(B) Injection rates in the three cases during injection of first 10000 seconds.

Reservoir modeling and Results

Influence of proppant embedment

recall

→ Proppant embedment *h*

Permeability distribution for different

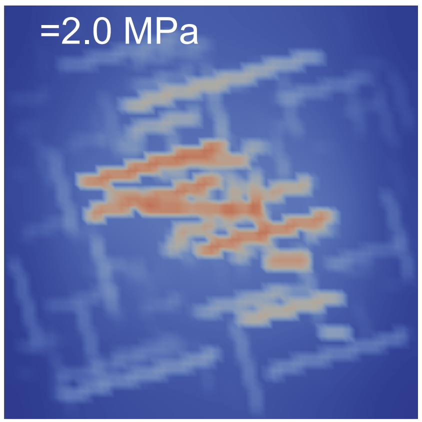

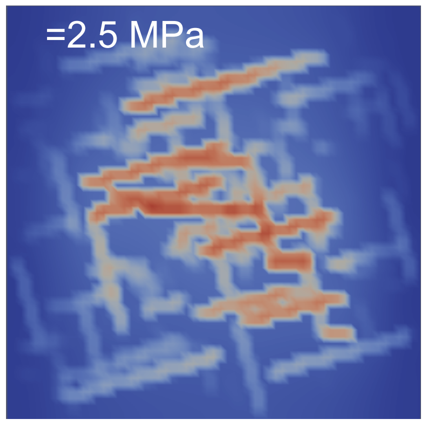

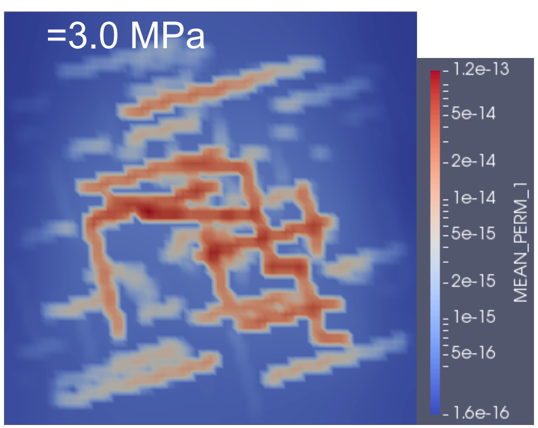

Before injection
Maximum of fracture permeability increases from m^2 to m^2

After 30-day injection
Maximum of fracture permeability increases from m^2 to m^2

Saturated fracture volume for different Cohesion

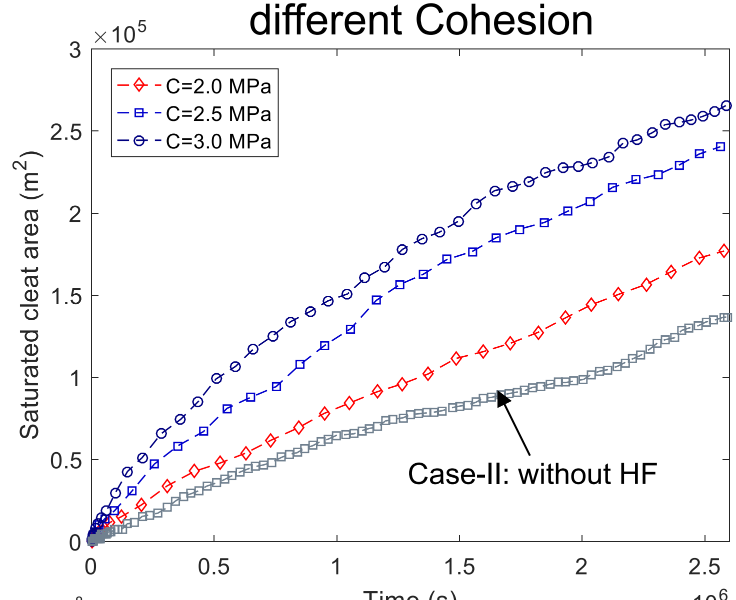

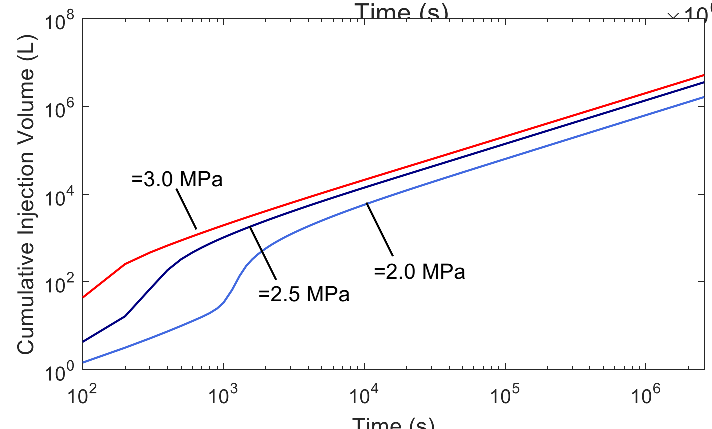

Reservoir modeling and Results

Production estimation

(*Saurabh 2018*)

where MY is methane yields in unit of mmol/g. m is the constant of proportionality, equal to one here. K (mmol/g) is the carrying capacity of the environment, P_0 (mmol/g) is the initial population in the environment, t is time and r (hr^{-1}) is the growth rate coefficient.)

Comparison between the production models and experimental data.

	Model #1 (Green 2008)	Model #2 (Bi 2018)
P_0	0.013	0.008
K	0.165	0.70
r	0.0066	0.0059

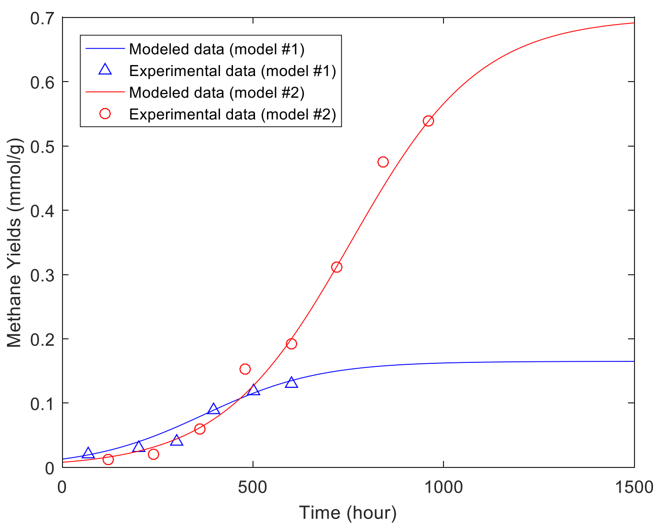

Influence of nutrient concentration

)=

(*Bi et al., 2017*)

where C1=Ethanol, C2=Methanol, C3=Isopropanol, C4=Sodium acetate

The optimal value for ethanol, methanol, 2-propanol and sodium acetate was 27, 50, 10 and 100 mM, respectively.

Therefore,

where MYR is the methane yield ratio, defined by

Production estimation

Model #1

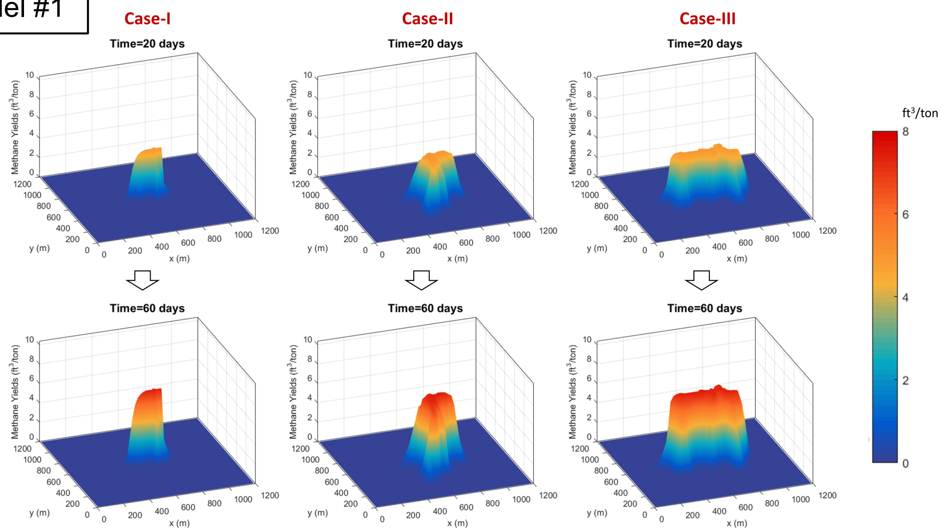

Model #2

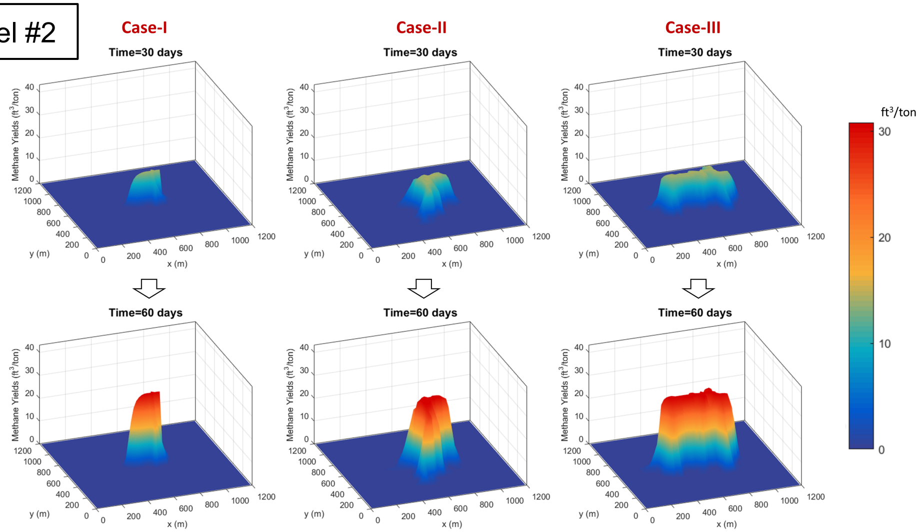

Model #1: baseline case (data extrapolated from *Green 2008*)
Model #2: optimal case (data extrapolated from *Bi 2018*)

The estimation of cumulative methane yields under different scenarios

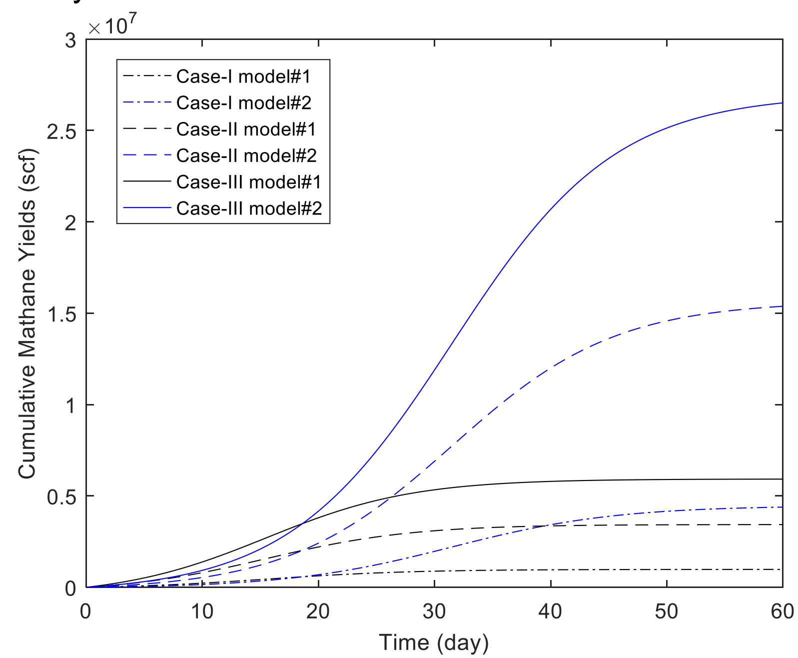

Reservoir modeling and Results

Influence of boundary condition

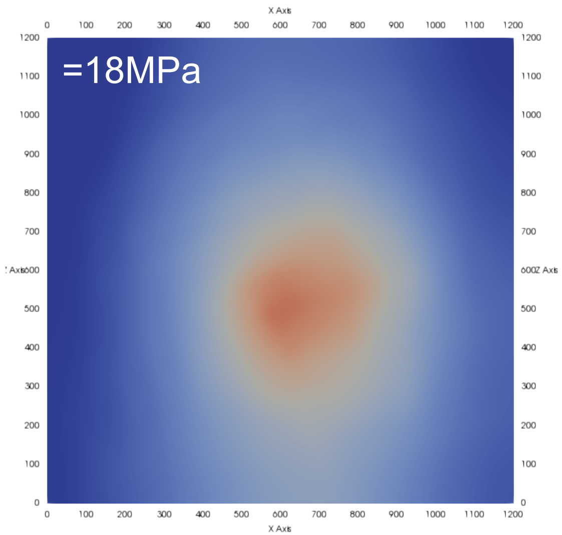

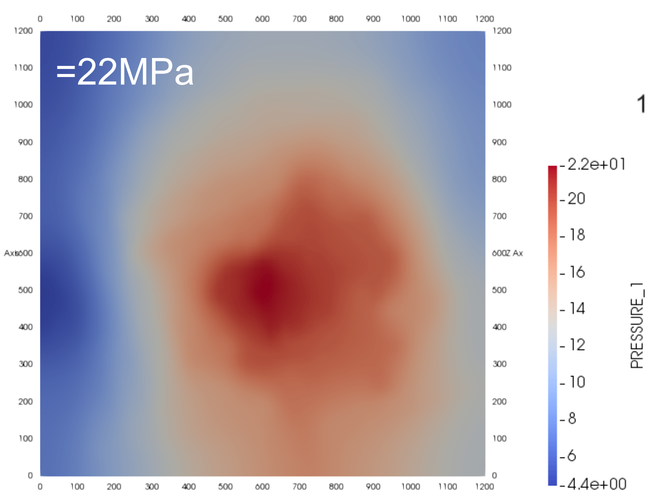

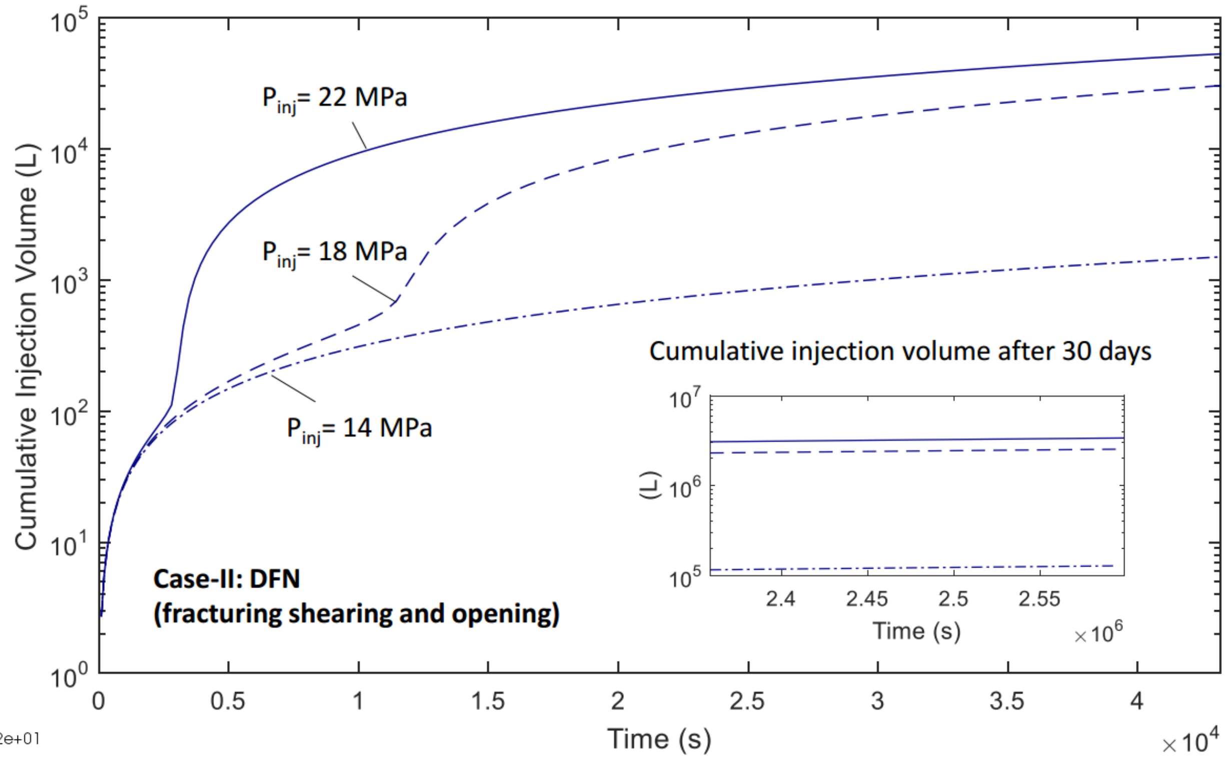

Nutrient will sweep more fracture volume when injection pressure is over confining stress

Conclusions

1. In this study, a field-scale numerical simulation using an **equivalent multi-continuum method** is established to define the effectiveness of nutrient delivery in a self-developed program TFReact. The complex fracture pattern existing in coal is represented by an overprinted **discrete fracture network (DFN)** to depict natural heterogeneity and anisotropy of fracture permeability in the CBM reservoir.

2. With small proppant embedment, the **propped hydraulic fractures** provide the most effective pathway for aqueous mineral transport. The pre-existing fracture network also plays a significant role in enhancing nutrient delivery. After comparing SCA and cumulative injection volumes in the three cases, it can be inferred that **hydraulically stimulated fracture pathways**, especially when connecting natural fracture network, will optimally deliver soluble nutrient remote from the injection well,

3. Two production models show the maximum methane yields of 7.36 ft^3/ton and 30.69 ft^3/ton, respectively. The cumulative methane yields after 60 days in the optimal case is MCF, about 6 folds larger than the case where nutrient is only diffused by matrix.